Universidade de Aveiro Departamento de Física,
2020

João Pedro Dias Rodrigues

A Study of possibilities beyond the Standard Model

o júri / the jury

presidente

Margarida Facão
Professora Auxiliar do Departamento de Física da Universidade de Aveiro

vogais

António Morais
Investigador Pos-doc do Departamento de Física da Universidade de Aveiro

Nuno Castro?
Professor at the University of Minho. Researcher at LIP and ATLAS experiment at CERN.

agradecimentos / acknowledgements

Honestamente acho que isto vai ter que ser escrito antes da entrega

Honestly this will be written in english translated poorly from above :)

Resumo

É impossível debater que o surpreendente sucesso do modelo padrão de física de partículas o faz um dos maiores sucesso da ingenuidade humana, no entanto, apesar de o modelo padrão descrever com grande detalhe todas as partículas observadas e as suas interações e conseguir tratar um grande número de fenomeno físicos onde era esperado encontrar falhas, tudo numa estrutura bem motivada, este é considerado incompleto.
Introduzir motivação para a falha do SM.
Introduzir motivação para mais Higgs.
Introduzir motivação para o BLSM
Introduzir motivação para o 3HDM
Tocar nas conclusões??

Abstract This part will be in English. Translated from above.

Contents

List of Figures

List of Tables

0.4 Labels

A paragraph or text to be added later
A mistake or a question that is likely wrong
A comment or doubt to ask or check
Excess? Probably will cut, waiting for advice

Chapter 1

Introduction

Modern study of particle physics is often taught trough the Standard Model (SM) of particle physics. The SM has thus far the best descriptor ~~for~~ the experimentally observed spectra of particles and their interactions at all current prob scales. And ~~In~~ 2012 a resonance was discovered in the LHC that seems to confirm the existence of it's pr ed particle, the Higgs n, finally completing the Model and proving the existence of the Higgs mechanism.

The history of the SM is a interesting one, and with it, scientists combined three of the four fundamental forces of nature in a very well motivated framework, making it one of the most monumental achievements in physics.

However, despite all these successes SM still lacks a strong theoretical explanation for several experimental observations. To name a few, firstly, the SM can not account for one of the most important cosmological discoveries of the century , observed troug avitational lensing, the existence of dark matter. This is a fundamental flaw since the SM lacks a possible dark matter candidate, or dark particle.

Secondly, the SM lacks an stification for the existence of baryon asymmetry in the universe, i.e. why is the universe primarily made of matter rather than anti-matter. Although note that the Electroweak baryogenesis (EWBG) remains a theoretically possible scenario for explaining the cosmic baryon asymmetry, a scenario viable in the SM framework. Is this stil true?

As its name suggests, EWBG refers to a mechanism that produces an asymmetry in the density of baryons decaying during the electroweak phase transition. This puts some requirements on the composition of the universe but would imply that all matter anti-matter asymmetry is created during the time when the Higgs field is settling into it's new vacuum expectation value (VEV). Should I remove this paragraph?

Thirdly, the SM has peculiar oddities in the fermion sector in the form of unjustified mass and mixing hierarchies. This is usually refereed to as the *flavour problem* and is considered a big drawback of the SM. Specifically, we observe the top quark to be five order of magnitudes heavier the up quark, and eleven orders of magnitude than the observed neutrino masses. These high differences are thought to be too large to be simply "nature", so a physical property that would justify such gap is a desired property of most Beyond the Standard Model (BSM) frameworks.

Fourth, note neutrino masses are not included in the SM. Although there are precise oscillation measurements that measure masses in the eV range with precise mixing in between 3 different generations of neutrinos.

These are just some of the typical justifications given to explore possible BSM scenarios. The holy grail of which would be a model that include all these problems in a properly motivated framework that addresses these and many more cosmological, gravitational, and phenomenological problems.

However, as of late the research in possible BSM scenarios as become progressively harder to perform given that the available space for new physics gets reduced by each successful experiment. Chief among these experiments is the Large Hadron Collider (LHC), whose large amount of collect data over these past years is setting more and more stringent bounds on viable parameter spaces of popular BSM scenarios. And as available space for new physics decreases it becomes more challenging to reveal remaining space without falling within the possibility of fine tuning our model.

How to properly explain what fine tunning is? Should I?

Note, that the SM has shown increasingly puzzling consistence with most constraints that were initial believed to be a possible gateway to new physics (NP) or that would diverge from it. Thus, the search continues for hints at possible directions to complete the SM. I should mention flavour changing and how the SM needs a very strange matrix for that to happen

Conventionally, BSM searches in these multi-dimensional parameter spaces have often been made in large computer-clusters with use of several weeks of computational time trough simple Monte-Carlo methods. Although this is the basis of the work presented here a effort was made to incorporate new machine learning routines trough the initial building of smaller learning sets trough conventional methods. Unfortunately this wasn't accomplished in this work due to the expectational setbacks felt this year.

During this work we shall do a small expedition into possible BSM scenarios. However we will start by laying down the fundamental basis for this BSM discussion by presenting a short overview of the SM, then we discuss possible extensions and alterations of the SM. First by presenting the B-L-SM model, a simple unitary extension based on a apparently accidental symmetry of the SM. And then by moving on to a more complex model with additional Higgs doublets fields as a attempt to present a framework that addresses the *flavour problem*. Note while the minimally structure of the Higgs sector postulated by the SM is not a immediate contradiction of measurements. It is not manifestly required by the data. And in fact a extended scalar sector is often desired to deal with many of it's shortcomings despite the relatively tight bounds on Higgs boson couplings to SM gauge boson and heavy fermions. We give a higher repute to the Higgs Sector since fermion masses and mixing patterns relate often to the specific structure of the Higgs sector. Also, the addition of new scalars offer a large playground for collider experimentation and often offer the inclusion of new neutrino physics.

The models with more than one Higgs doublet also addresses the observed charge parity CP violation. With the drawback of potentially having large Flavour Changing Neutral Currents (FCNCs). These FCNCs are undesirable at least in large number given observations, although multiple Higgs Doublets could include these diagrams at tree-level, making them very problematic. The mechanisms that suppress this should be presented.

In short two particular multi-Higgs models will be presented in this work a phenomenological study of a 3 Higgs Doublet model (3HDM) with softly broken $\mathrm{U}(1)_\times \mathrm{Z}_2$ symmetry and a simple Unitarity, U(1), extension of the SM based on the apparent Baryon minus Lepton symmetry (B-L-SM). We'll investigate what can be learned from these models and what other physical experiments constrict them.

Chapter 2

The Standard Model of Particle Physics

2.1 Motivation

Has stated, it is hard to question the validity of the SM as a successful, at least approximate, framework with whom to describe the phenomenology of Particle Physics up to the largest energy scales probed by collider measurements so far, although some inconsistencies remain and must be addressed. The SM was proposed in the nineteen sixties by Glashow, Salam and Weinberg and since it has been extensively tested. Both in contemporary direct searches for new physics and indirect probes via e.g. flavour anomalies and precise electroweak parameter measurements in proton-electron collisions.

The path to the formulation of the SM came from previous principles relating to symmetries in nature, specifically symmetry in physical laws. In fact, much in modern physics can be attributed to Emmy Noether's work. She deduced, trough her first theorem, that if the action in a system is invariant under some group of transformations (symmetry), then there exist one or more conserved quantities (constants of motion) which are associated to these transformations.

Physicist took this idea and were led to the fundamental question behind the SM, is it possible that upon imposing to a given Lagrangian the invariance under a certain group of symmetries to reach a given form for it's the dynamics? These dynamics would be in our context, particle interactions. This train of thought first led to Quantum Electrodynamics (QED), then Quantum Chromodynamics (QCD) and finally the SM.

We can quote Salam and Ward:

"Our basic postulate is that it should be possible to generate strong, weak and electromagnetic interaction terms (with all their correct symmetry properties and also with clues regarding their relative strengths) by making local gauge transformations on the kinetic energy terms in the free Lagrangian for all particles."

We are glossing over a lot of complexity here, and for the SM to be properly formulated additional concepts would be required. In the case of weak interactions, the presence of very heavy weak gauge bosons require the new concept of spontaneous breakdown of the gauge symmetry and the Higgs mechanism. While the concept of asymptotic freedom played a crucial role to describe perturbatively the strong interaction at short distances.

2.2 Internal symmetry of the Standard Model

The SM is a "standard" QFT gauge theory, that is to say, it is manifestly invariant under a set of field transformations. The SM gauge group, $\mathcal{G}_{SM}$, is seen in,

$$\mathrm{SU}(3)_\mathrm{c} \times \mathrm{SU}(2)_\mathrm{L} \times \mathrm{U}(1)_\mathrm{Y} \quad . \tag{2.1}$$

Here we have, first, the $\mathrm{SU}(3)_\mathrm{c}$ group corresponding to quantum chromodynamics (QCD), responsible for the strong force, this symmetry will remain unbroken by the electroweak VEV. Secondly, we have the $\mathrm{SU}(2)_\mathrm{L} \times \mathrm{U}(1)_\mathrm{Y}$ portion that will be broken by the Higgs mechanism into $\mathrm{U}(1)_\mathrm{Q}$, the electromagnetic gauge symmetry.

Each particle stems from a field that is charged in a particular manner on each of these groups, making the charge triplets we will come to later define. Given the invariance under the group in eq. 2.1, we will show it is impossible have any field that is charged have a explicit mass term. This chapter will focus on how the mass of particles is generate trough the Higgs mechanism. And offer a brief discussion of flavour physics in the SM and how flavour changing currents can point to New Physics (NP).

Gauge Group numbers

The full set of quantum numbers in all the SMs fields are described in the tables 2.1 and 2.2, with the color charge, weak isospin number and the hypercharge are given by their ordered entries in each triplet.

Table 2.1: Gauge and Scalar fields dimensions in the SM

Fields	Spin 0 field	Spin 1 Field	$SU(3)_C \times SU(2)_L \times U(1)_Y$
Gluons	$\times$	g	(8,1,0)
A bosons	$\times$	A^i	(1,3,0)
B bosons	$\times$	B	(1,1,0)
Higgs field	$(\phi^\pm, \phi^0)$	$\times$	(1,2,1)

Table 2.2: Fermion field dimensions in the SM

Fields	Spin $\frac{1}{2}$ Field	$SU(3)_C \times SU(2)_L \times U(1)_Y$
Quarks (3 gen.)	$Q = (u_L, d_L)$	$(3, 2, \frac{1}{3})$
	u_R	$(3, 1, \frac{4}{3})$
	d_R	$(3, 1, -\frac{2}{3})$
Leptons (3 gen.)	$(L = (\nu_{e_L}, e_L)$	$(1, 2, -1)$
	e_R	$(1, 1, -2)$

From here, given the gauge group in, eq. 2.1 and accounting for the charges and fields, we can derive the form of the SM's Lagrangian. These gauge groups are composed of 12 generators and are governed by the following algebra,

$$[L_a, L_b] = i f_{abc} L_c \quad [T_a, T_b] = 1\epsilon_{abc} T_c \quad [L_a, T_b] = [L_a, Y] = [T_b, Y] = 0 \tag{2.2}$$

where for the $\mathrm{SU}(3)_\mathrm{c}$ triplets, $L_a = \frac{\lambda_a}{2}$, $(a = 1, ..., 8)$ contrary to $\mathrm{SU}(3)_\mathrm{c}$ singlets where, $L_a = 0$. As for the $\mathrm{SU}(2)_\mathrm{L}$, we have $T_i = \frac{\sigma_i}{2}$, $(i = 1, 2, 3)$, being that again for singlets $T_b = 0$. Y is the generator of $U(1)_Y$. The symbols λ_a and σ_i represent the Gell-Mann and Pauli matrices respectively.

2.2.1 Fields, Particles and Lagrangian of the SM

From these fields the physical states of the SM, it's particle spectrum, is composed by, first, the gauge bosons, the weak force carriers, $W^{\pm}$ and Z bosons, and the photon γ, the electromagnetic interaction messenger and the strong force mediators, the gluons, g, as well, of course, by the matter particles, the fermions, composed by the quarks and leptons.

Leptons and quarks are organized in three generations each, with 2 pairs by each generation leading to 6 different particles for each. For quarks we have the up and down for the first generation, charm and strange for the second as well as top and bottom for the third one. Similarly, there are 6 types of leptons, the charged ones, electron, muon and tau, and the associated neutrinos. These are represented in different manners, being that the quarks are represented by the letters (u, d, c, s, t, b) while leptons as $(e, \nu_e, \mu, \nu_\mu, \tau, \nu_\tau)$.

Fermions are half integer spin particles half of which have electrical charge (except the neutrinos). While quarks interact via the weak, electromagnetic and strong forces, the charged leptons only feel the electromagnetic and weak forces and the neutrinos are weakly interacting.

A physical fermion is composed of a left-handed and a right-handed field. While the left transform as $SU(2)_L$ doublets and can be written as,

$$L^i = \begin{pmatrix} \nu_{e_L} \\ e_L \end{pmatrix}, \begin{pmatrix} \nu_{\mu_L} \\ \mu_L \end{pmatrix}, \begin{pmatrix} \nu_{\tau_L} \\ \tau_L \end{pmatrix} \quad \text{and} \quad Q^i = \begin{pmatrix} u_L \\ d_L \end{pmatrix}, \begin{pmatrix} c_L \\ s_L \end{pmatrix}, \begin{pmatrix} t_L \\ b_L \end{pmatrix} \quad , \tag{2.3}$$

where the i index stands for generation, often designed as the flavour index, the latter are $\mathrm{SU(2)_L}$ singlets and can be simply represented as

$$e^i_R = \{e_R, \mu_R, \tau_R\}, \quad u^i_R = \{u_R, c_R, t_R\}, \quad d^i_R = \{d_{e_R}, s_{e_R}, b_{e_R}\} \quad , \tag{2.4}$$

note also that the quarks form triplets of $\mathrm{SU(3)_C}$ whereas leptons are colour singlets. The Higgs boson also emerges from an $\mathrm{SU(2)_L}$ doublet with the form,

$$H = \begin{pmatrix} \phi^1 + i\,\phi^2 \\ \phi^3 + i\,\phi^4 \end{pmatrix} \quad , \tag{2.5}$$

Here we see the four components that correspond to the respective degrees of freedom of the Higgs Field. After the process of SSB of the SU(2)˙L $\times\, U(1)_Y$ group the charges of the fermions along their QCD and QED numbers become,

Table 2.3: Quark and Lepton charges

	$\mathrm{SU(3)_C}$	$\mathrm{U(1)_Q}$
Up type quarks (u, c, t)	3	2/3
Down type quarks (d, s, b)	3	-1/3
Charged leptons (e, μ, τ)	1	-1
Neutrinos $(\nu_e, \nu_\mu, \nu_\tau)$	1	0

Lagrangian formulation

Given the SM gauge groups and charges seen in 2.1 the covariant derivative, D_μ, will read as,

$$D_\mu = \partial_\mu - ig_S\tau^a G^a_\mu - igT^i A^i_\mu - ig'YB_\mu \quad , \tag{2.6}$$

We can expect 3 different type of couplings, g_s related to the $\mathrm{SU(3)_C}$ subgroup, g to the $\mathrm{SU(2)_L}$ and g' to $\mathrm{U(3)_Y}$. The associated canonical field strength tensors would be,

$$G^{\mu\nu}_a = \partial^\mu G^\nu_a - \partial G^\mu_a - g_s f_{abc} G^\mu_a G^\nu_b \tag{2.7}$$
$$W^{\mu\nu}_a = \partial^\mu W^\nu_a - \partial^\nu W^\mu_a - g\epsilon_{abc} W^\mu_b W^\nu_c \tag{2.8}$$
$$B^{\mu\nu} = \partial^\mu B^\nu - \partial^\nu B^\mu \tag{2.9}$$

It is often convenient to present the SMs Lagrangian in portions, usually divided in three sections,

$$\mathcal{L}_{SM} = \mathcal{L}_{kin} + \mathcal{L}_{Yuk} + \mathcal{L}_{\phi} \tag{2.10}$$

Where we have the kinetic portion of the SM terms, $\mathcal{L}_{kin}$, responsible for free propagation of particles, the Yukawa portion, $\mathcal{L}_{Yuk}$ corresponding to interactions of particles with the Higgs Boson, and finally the $\mathcal{L}_{\phi}$ scalar potential. The full kinetic portion of the SM read,

$$\begin{aligned}\mathcal{L}_{kin} = &-\frac{1}{4}G_a^{\nu\mu}G_{a\,\nu\mu} - \frac{1}{4}W_a^{\nu\mu}W_{a\,\nu\mu} - \frac{1}{4}B^{\nu\mu}B_{\nu\mu} \\ &- i\overline{Q_{L_i}}\not{D}Q_{L_i} - i\overline{u_{R_i}}\not{D}u_{R_i} - i\overline{d_{R_i}}\not{D}d_{R_i} - i\overline{L_{L_i}}\not{D}L_{L_i} - i\overline{e_{R_i}}\not{D}e_{R_i} \\ &- (D_\mu H)^\dagger(D^\mu H)\end{aligned} \tag{2.11}$$

Where $\not{D}$ is the Dirac covariant derivative, $\gamma^\mu D_\mu$. From the last line Eq. 2.11 and with Eq. 2.6 we will present how the Generators A_μ^i and B_μ give rise to the weakly interacting vector bosons $W^\pm$ and Z^0 and the electromagnetic vector boson γ. Contrary to the color sector, where the eight generators G_μ^a simply correspond to eight gluons g a mediating strong interactions. Maybe move this to where it actually is written While the scalar potential part

$$\mathcal{L}_\phi = -\mu^2 HH^\dagger - \lambda(HH^\dagger)^2 \tag{2.12}$$

Finally the Yukawa portion of the Lagrangian would be written as,

$$\mathcal{L}_{Yuk} = Y_{ij}^u\overline{Q_{L_i}}u_{R_j}\tilde{H} + Y_{ij}^d\overline{Q_{L_i}}d_{R_j}H + Y_i^e j\overline{L_{L_i}}e_{R_i}H + h.c. \tag{2.13}$$

Here we have, $\tilde{H} = i\sigma_2 H$. It is due to the Yukawa interactions between the Higgs and the fermions and leptons that these acquire their masses once the Higgs settles into his VEV. same as before

2.3 The Higgs mechanism and the mass generation of the Gauge bosons

From what was defined above, we can now study the process SSB by which,

$$\mathrm{SU(2)_L \times U(1)_Y \to U(1)_Q} \tag{2.14}$$

and carry trough to the Higgs Mechanism. Enabling us to find the real physical states of the gauge bosons and the origin of their mass. Let us then consider the part of the Lagrangian containing the scalar covariant derivatives, the scalar potential and the gauge-kinetic terms:

$$\mathcal{L}_{Gauge} \supset (D_\mu H)(D^\mu H)^\dagger - \mu^2 H^\dagger H - \lambda(H^\dagger H)^2 - \frac{1}{4}W_a^{\nu\mu}W_{a\,\nu\mu} - \frac{1}{4}B^{\nu\mu}B_{\nu\mu} \tag{2.15}$$

We expect a phase shift to occur, namely one that ensures $\mu^2 < 0$ while at the same ensuring that the field now explicitly breaks the $\mathrm{SU(2)_L \times U(1)_Y}$. For this to happen we expect the shifted squared value of the Higgs field to be,

$$(H^\dagger H) = \frac{-\mu^2}{2\lambda} = \frac{1}{2}v \quad , \tag{2.16}$$

This VEV, called the electroweak VEV, is experimentally measured to be $v \approx 246$ GeV. The choice of vacuum can be aligned in such a way that we have,

$$H_{min} = \frac{1}{\sqrt{2}}\begin{pmatrix}0\\ v\end{pmatrix} \quad . \tag{2.17}$$

Given that now the $SU(2)_L \times U(1)_Y$ symmetry is broken down to $U(1)_Q$ we jump from a scenario where there were four generators, which are $T^{1,2,3}$ and Y, to, after the breaking, having solely one unbroken combination that is $Q = (T^3 + 1/2)$ associated to the electric charge. This means that in total we will have three broken generators, thus, from Goldstone Theorem, there would have to be created three massless particles.

These Goldstones modes however can then be parametrized as phases in the field space and then can be "rotated away" in the physical basis, leaving us with a single physical massive scalar, the Higgs boson. Note that, with this transformation we are removing three scalar degrees of freedom. However, they cannot just disappear from the theory and will be absorbed by the massive gauge bosons. In fact, a massless gauge boson contains only two scalar degrees of freedom (transverse and polarization). Meanwhile, a massive vector boson has two transverse and a longitudinal polarization, i.e., three scalar degrees of freedom. So, as we discussed above, while before the breaking of the EW symmetry we have four massless gauge bosons, after the breaking we are left with three massive ones. This means that there are three extra scalar degrees of freedom showing up in the gauge sector. It is then commonly said that the goldstone bosons are "eaten" by the massive gauge bosons and the total number of scalar degrees of freedom in the theory is preserved. Therefore, without loss of generality, we can rewrite the Higgs doublet as

$$\begin{pmatrix} G_1 + iG_2 \\ v + h(x) + iG_3 \end{pmatrix} = H(x) \to H(x) = \frac{1}{\sqrt{2}} \begin{pmatrix} 0 \\ v + h(x) \end{pmatrix} \quad . \tag{2.18}$$

Once the Higgs doublet acquires a VEV, the Lagrangian (2.15) can be recast as:

$$\begin{aligned} \mathcal{L}' =& \frac{1}{2}\partial_\mu h \partial^\mu h - \frac{1}{2}(2v^2\lambda)h^2 - \frac{1}{4}W_a^{\nu\mu}W_{a\,\nu\mu} - \frac{1}{4}B^{\nu\mu}B_{\nu\mu} \\ &+ \frac{1}{8}v^2 g^2 (A^1_\mu A^{1,\mu} + A^2_\mu A^{2,\mu}) + \frac{1}{8}v^2(g^2 A^3_\mu A^{3,\mu} + g'^2 B_\mu B^\mu - 2g^2 g'^2 A^3_\mu B^\mu) \quad , \end{aligned} \tag{2.19}$$

A few things become obvious first, we have a lot of mass terms most stemming from the squared gauge fields and a lonesome squared mass term belonging to the real scalar field we know to be the Higgs field. This makes the Higgs boson mass in the SM to be given by,

$$M_h = (2v^2\lambda) \quad . \tag{2.20}$$

To obtain masses for the gauge bosons we need to rotate the gauge fields to a basis where the mass terms are diagonal. First, it is straightforward to see that the electrically charged eigenstates are given by

$$W^\pm_\mu = \frac{1}{\sqrt{2}}(A^{(1)}_\mu \pm iA^{(2)}_\mu) \quad , \tag{2.21}$$

meaning that the mass of the W bosons is,

$$M_{W^\pm} = \frac{1}{2}vg \quad . \tag{2.22}$$

The situation becomes a bit more complicated for the second term in (2.19) due to a mixing between A^3_μ and B_μ. In the gauge eigenbasis the mass terms read

$$\begin{pmatrix} A^3_\mu & B_\mu \end{pmatrix} \cdot \frac{1}{4}\nu^2 \begin{pmatrix} g^2 & -gg' \\ -gg' & g'^2 \end{pmatrix} \cdot \begin{pmatrix} A^3_\mu \\ B_\mu \end{pmatrix} \quad , \tag{2.23}$$

which can be diagonalized to obtain

$$\begin{pmatrix} A_\mu & Z_\mu \end{pmatrix} \begin{pmatrix} 0 & 0 \\ 0 & \frac{1}{2}v\sqrt{g^2 + g'^2} \end{pmatrix} \begin{pmatrix} A^\mu \\ Z^\mu \end{pmatrix} \quad , \tag{2.24}$$

we identify the eigenvector associated to the eigenvalue 0 to the photon and the massive one, $M_Z = \frac{1}{2}v\sqrt{g^2 + g'^2}$, to the Z boson. Such eigenvectors can be written as

$$A_\mu = \cos(\theta_\omega)B_\mu + \sin(\theta_\omega)A^3_\mu \quad , \tag{2.25}$$

$$Z_\mu = -\sin(\theta_\omega)B_\mu + \cos(\theta_\omega)A^3_\mu \quad , \tag{2.26}$$

where θ_w is the so called Weinberg mixing angle and is defined as,

$$\cos(\theta_\omega) = \frac{g}{\sqrt{g^2 + g'^2}} \quad , \tag{2.27}$$

thus clearly showing the massless photon along with a massive Z boson with mass $M_Z = \frac{1}{2}\nu\sqrt{g^2 + g'^2}$. So we conclude our exploration of the electroweak sector with all the correct massive spectrum observed and its origin discussed.

2.4 Fermion Masses in the SM and Quark mixing

As referenced, given the charges of the fermion and lepton fields we cannot construct a gauge invariant theory with explicit mass terms for leptons. The mass of these particles are generated through quark couplings to the Higgs, by the Higgs mechanism.

$$\mathcal{L}_{Yuk} = Y^u_{ij}\overline{Q_{L_i}}u_{R_j}\tilde{H} + Y^d_{ij}\overline{Q_{L_i}}d_{R_j}H + Y^e_i j\overline{L_{L_i}}e_{R_i}H + h.c. \tag{2.28}$$

where $Y^{e,u,d}$ stand for the Yukawa matrices, these are generic 3×3 complex non-dimensional coupling matrices, H is the Higgs field with $\tilde{H}$ retaining it's previous definition, i, j are the standard generation indices, Q_{L_i},are the left handed quark doublets, while d_R and u_R are the corresponding right-handed down and up quark singlets respectively in the weak eigenstate basis. The Yukawa matrices contain some parameters that are not observable (unphysical) since they can be absorbed by redefinitions of the real fermion fields. Note that the increasing masses seen in each generation depend directly on the term hierarchy of the Yukawa terms. This means that the mass of all particles directly relate to how strongly they each interact with the Higgs boson. If you then take into account the real masses e.g. for the leptons, the tau mass is in the GeV range while the electron's is in the 0.1 MeV range. These translate to very different couplings for each flavour. This hierarchy is unjustified in the SM. Has the Higgs field settles into the electroweak VEV Eq. 2.28 yields mass terms for the quarks and leptons. The Higgs mechanism generates the mass for all the fermionic and leptonic particles except for neutrinos, this is due to the SM not containing right handed neutrinos, i.e we can't build terms that would lead to neutrino masses. The addition of right handed neutrino fields is very commonly made in BSM cenarios. To reach the physical states starting from the weak eigenbasis you must diagonalize the yukawa matrices. This is done through a bi-unitary transformation. We can write these transformation under the form,

$$M^{u,d,e}_{\text{diag.}} = U^{u,d,e}_L Y^{u,d,e} U^{u,d,e}_R \frac{v}{\sqrt{2}} \tag{2.29}$$

where v stands for the electroweak VEV. And $U^{u,d,e}_L$ and $U^{u,d,e}_R$ are the required 6 unitary matrices. The charged lepton Yukawa matrix can always be made real and positive through a bi-unitarity transformation. Meaning the Yukawa matrix for the leptons contains only 3 real physical parameters that correspond to the Lepton masses. Naturally we can invert Eq. 2.29, returning equations for the yukawa matrices as,

$$\begin{aligned} Y^u_{ij} &= \frac{\sqrt{2}}{v}(U^u_L M^u_{\text{diag.}} U^u_R)_{ij} \\ Y^d_{ij} &= \frac{\sqrt{2}}{v}(U^d_L M^d_{\text{diag.}} U^d_R)_{ij} \end{aligned} \tag{2.30}$$

We can see this change creates mass terms for physical quark fields by replacing the result of eq. 2.30 in the Yukawa portion of the Lagrangian (Eq. 2.13).

$$
\begin{gathered}
\mathcal{L}_{Yuk} \supset -\frac{\sqrt{2}}{v} d_{L\,i}\, d_{R\,j} - \frac{\sqrt{2}}{v} u_{L\,i}\, u_{R\,j} + h.c. \\
\Downarrow \\
-(U_L^d m^d_{\text{diag.}} U_R^d)_{ij} d_{L\,i}\, d_{R\,j} - (U_L^u m^u_{\text{diag.}} U_R^u)_{ij} u_{L\,i}\, u_{R\,j} \\
\Downarrow \\
-m^d_{\text{diag.}_j} d'_{L\,i}\, d'_{R\,j} - m^u_{\text{diag.}_j} u'_{L\,i}\, u'_{R\,j}
\end{gathered}
\tag{2.31}
$$

where the primed fields are the quark fields in the mass basis, defined as,

$$
\begin{aligned}
d'_{L,R} &= U^d_{L,R} d_{L,R} \\
u'_{L,R} &= U^u_{L,R} u_{L,R}
\end{aligned}
\tag{2.32}
$$

As a result of this redefinition we can now look at the gauge interactions to see that a charge current appears where $W^{\pm}$ couple to the physical u'_{L_j} and d'_{L_j}. The coupling of the of fermions to their respective gauge fields changes by virtue of the fact only left handed Quarks are $SU(2)_L$ doublets, if we expand the up and down quark fields on the kinetic portion of the Lagrangian,

$$
\begin{aligned}
\mathcal{L}_{ferm} \supset & \frac{1}{2}\overline{u'_L}\gamma^{\mu}\left(g' Y_L B_{\mu} + g W^0_{\mu}\right)\left(U^u_L U^{u\dagger}_L\right) u'_L - \frac{1}{\sqrt{2}} g \overline{u'_L}\gamma^{\mu}\left(U^u_L U^{d\dagger}_L\right) d'_L W^+_{\mu} \\
& - \frac{1}{\sqrt{2}} g d'_L \gamma^{\mu}\left(U^u_L U^{d\dagger}_L\right) u'_L W^-_{\mu} + \frac{1}{2}\overline{d'_L}\gamma^{\mu}\left(g' Y_L B_{\mu} - g W^0_{\mu}\right)\left(U^d_L U^{d\dagger}_L\right) d'_L
\end{aligned}
$$

We can trough the use of the properties of unitary matrices, namely, $\mathrm{U}^{u,d}_{L,R}\mathrm{U}^{u,d\dagger}_{L,R} = 1$, note that the interactions with the neutral bosons remain the same in the mass basis. However we can see that the charged currents are affected by this change. Therefor here we define the Cabibbo-Kobayashi-Maskawa (CKM) matrix, as $V_{CKM} = U^u_L U^{u^{\dagger}}_R$ and write the sensitive terms,

$$
\mathcal{L}_{kin} \supset \frac{1}{\sqrt{2}} g \overline{u}'_L \gamma^{\mu} V_{CKM} d'_L W^+_{\mu} + h.c.
\tag{2.33}
$$

The CKM matrix, is a 3×3 unitary matrix. It is a paramatrization of the three mixing angles and CP-violating KM phase. There are many possible conventions to represent the CKM matrix.

It is through this complex phase in the CKM matrix that the SM can account for the phenomena of $\mathcal{CP}$ violation. First observed in the famous K^0 decay into $\mu^+\ \mu^-$ ($CP = +1$ and $CP = -1$ respectively) that won the 1980 Nobel Prize. The discovery opened the door to questions still at the core of particle physics and of cosmology today. Not just the lack of an exact CP-symmetry, but also the fact that it is so close to a symmetry.

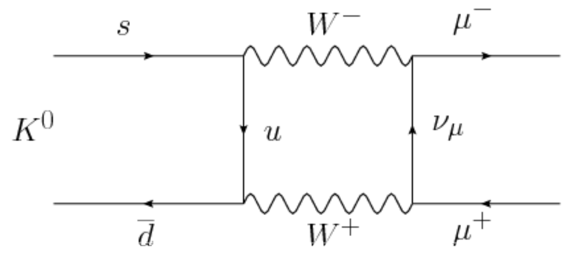

Figure 2.1: Box diagram describing $K^0_L \to \mu^-\mu^+$, through an intermediate u quark.

This is in fact a very interesting feature of the Standard Model, by consequence of the $\mathrm{SU(2)_L \times U(1)_Y}$ symmetry there are no interactions of the right handed unitary matrices and there for no mixing, coupling, or charged currents of right handed quarks, making them theoretically invisible to measurements.

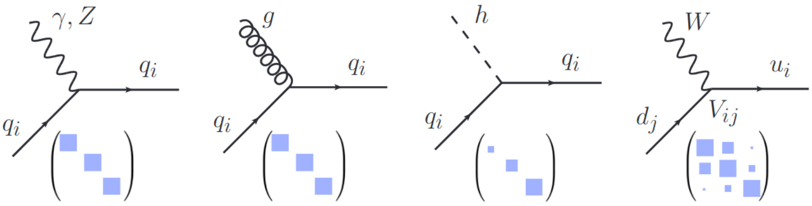

Figure 2.2: The Feynman diagrams for flavour conserving couplings of quarks to photon, Z boson, gluon and the Higgs (the first three diagrams), and the flavour changing coupling to the W (the last diagram). The 3×3 matrices are visual representations of couplings in the generation space, with couplings to γ ,Z, g flavour universal, the couplings to the Higgs flavour diagonal but not universal, and the couplings to W flavour changing and hierarchical.

The CKM matrix elements are fundamental parameters of the SM, so their precise determination is important, and reproducing the quark mixing parameter is fundamental for BSM searches.

2.5 Physical parameters

Should I introduce the physical paramater and count the 19 SM parameters?

2.5.1 Charged Flavour Currents vs. Neutral Flavour Currents

In the SM there is a very important distinction between flavour changing neutral and charged currents. Flavour Changing Neutral Currents (FCNCs) are processes in which the quark flavour changes, while the quark charge stays the same. The Flavour Changing Charged Currents (FCCCs) change both the flavour and the charge of the quark. A glimpse at the PDG booklet [ ] reveals that the probabilities for the two types of processes are strikingly different. The charged currents lead to the dominant weak decays, while the FCNC induced decays are extremely suppressed. Rounding the experimental results, and not showing the errors, a few representative decays are,

Table 2.4: FCCCs examples

$s \to u\mu^- \nu_\mu$	: Br $(K^+ \to \mu^- \nu) = 64\%$
$b \to c l^- \nu_l$	: Br $\left(B^- \to D^0 l \bar{\nu}_l\right) = 2.3\%$
$c \to u\mu^- \nu_\mu$	: Br $\left(D^\pm \to K^0 \mu^\pm \nu\right) = 9\%$

Table 2.5: FCNCs examples

$s \to d\mu^+\mu^-$	: Br $(K_L \to \mu^+\mu^-) = 7 \times 10^{-9}$
$b \to d\mu^+\mu^-$	: Br $(B^- \to K^{*-} l^+ l^-) = 5 \times 10^{-7}$
$c \to u l^+ l^-$	: Br $\left(D^0 \to \pi l^+ l^-\right) = 1.8 \times 10^{-4}$

The reason for such a striking difference is that in the SM the charged currents occur at tree level,while FCNCs are forbidden at tree level and only arise at one loop, see Fig. 3.

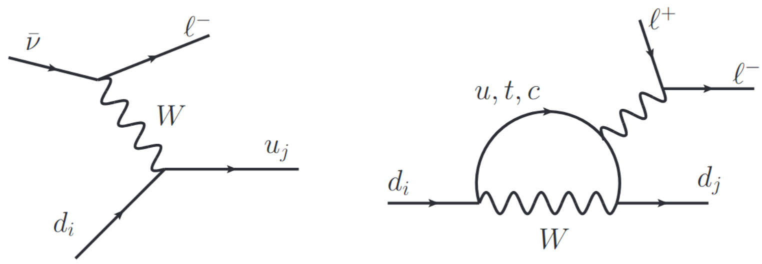

Figure 2.3: Representative tree level charged current diagram (left) and a loop induced FCNC diagram (right).

Furthermore, the FCNCs come suppressed by the difference of the masses of the quarks running in the loop, $m_j^2 - m_i^2$. This so called Glashow-Iliopoulos-Maiani (GIM) mechanism [ ] is a result of the fact that there is no flavour violation, if all the quark masses are the same.

Flavour as a Probe into New Physics

Now that we have introduced without great detail flavour physics we can briefly touch on why collider experiments have been sold a as a pathway to discovering new physics i.e. how deviation in rare decays could pin point exactly what is missing in the Standard Model.

Thanks to these large experiments we have many new observables in flavour physics, e.g. the branching ratios, asymmetries, distributions. There is also a plethora of different parent particles for each, as well as many instances of final states.

The abundance of observables is clearly illustrated by opening the handy Particle Data Group (PDG) book [Same ref as above]. Even the condensed version, the PDG booklet, clocks out at more than 170 pages.

The recipe seemed simple, identify processes that are rare in the SM and then search for deviations from the SM predictions. However thus far all but two processes are within experimental and theoretical bounds given by the SM. This refers to $b \to s\mu\mu$ and $b \to c\tau\nu$, these are showing over 4σ deviations from the their expected value.

If examined through V-A operators the NP scale of these 2 processes are both very different and very heavy, these would be something a kin to,

$$\mathcal{L}_{NP} \supset \frac{1}{\Lambda_{NP}} (\overline{Q}_i \gamma^\mu \sigma^A Q_j)(\overline{L}_k \gamma_\mu \sigma^A L_l) \tag{2.34}$$

To explain $b \to s\mu\mu$ transitions you would need a $\Lambda_{NP} \approx 3$ TeV while for $b \to c\tau\nu$ you would need a $\Lambda_{NP} \approx 30$ TeV. This is a strong indicator that some components are missing in our formulation like a new mediator for gauge interactions.

An advantage of the proposed NP scale contributions is that the required scale would avoid most experimental constraints. The FCNC diagram for the particular $b \to s\mu\mu$ channel can be seen in Fig 2.4,

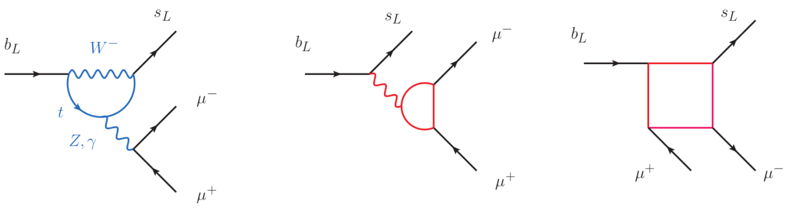

Figure 2.4: A representative SM diagram for $b \to s\mu\mu$ transition (left), and representative possible loop level NP contributions (middle and right).

The $b \to c\tau\nu$ flavour anomaly is similarly very clean theoretically [ ], and the disagreement with the SM predictions is also about 4 σ. However, the NP effect is large and often this means that the scale of NP needs to be low, and consequently the NP interpretations are often in conflict with the other constraints.

This means the most obvious candidates are ruled out. Theoretical bias would have been that the new charged currents are either due to a charged Higgs, H^+ , or a new vector boson, W', see Fig. 2.5.

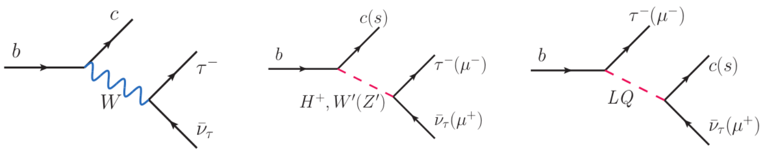

Figure 2.5: The SM diagrams for $b \to c\tau\nu$ transition (left), and the possible tree level NP contributions to $b \to c\tau\nu$ transition (middle and right).

Another prediction of the SM is that the rates for the $b \to se^+e^-$ and $b \to s\mu^-\mu^+$ transitions should be equal to each other. The SM prediction of Lepton Flavour Universality (LFU) is deeply engrained in the structure of the theory, since it is a consequence of the fact that the electroweak gauge group is the same for all three generations.

The prediction of LFU can be tested experimentally, also trough flavour physics, by theoretically clean observables such as the ratios of these flavour observables,

$$R_{K^*} = \frac{\mathrm{Br}(B \to K^*\mu^-\mu^+)}{\mathrm{Br}(B \to K^*e^-e^+)} \tag{2.35}$$

Another strong indicator of new physics is the fact the experimental value for this ratio is $R_{K^*} \approx 0.7$, violating LFU by $2.2 - 2.6\sigma$

The Future of Flavour Indirect Searches

The NP searches with rare decays, as well boost with the upcoming Belle II and LHC upgrades. Belle II expects to collect 50 times the Belle dataset. First collisions were seen in May 2018, and the first B physics run is expected in March 2019. While for the LHC, after upgrade II aims for roughly 100 times the present data set with an upgraded detector. Undoubtedly this improvement in sensibility will translate to a finer value for all measurable parameters at these experiments. We expect these anomalies then to go over the required 5σ in future experiments (Assuming of course, they are not statistical deviations).

2.6 Quantum chromodynamics

I should meantion the QCD part of the Lagrangian

I should explain what is asymptoic freedom and meantion that the strong force fades fast. Free quarks at high energies

Chapter 3

B-L-SM Model

Having discussed the Standard Model, we are ready to look at what might lie beyond it. In this chapter we introduce the minimal $\mathrm{U}(1)_{\mathrm{B-L}}$ gauge extension of the Standard Model named, the B-L-SM Model [2, 3, 4]. This is a model trough which we can explain neutrino mass generation via a simple see-saw mechanism, additionally, by virtue of the model containing two new physical particle states, specifically a new Higgs like boson H' and a Z' gauge Boson we can also address other phenomenology, such as deviations in electro-weak measurements, namely the $(g-2)_\mu$ anomaly. The discrepancy between the measured anomalous magnetic moment of the muon and the SM expected value [5].

Both the additional bosons are given mass primarily trough the spontaneous breaking of the $\mathrm{U}(1)_{\mathrm{B-L}}$ symmetry that gives it's name to the Model. This unitary group originates from the promotion of a accidental symmetry present in the SM, the Baryon number (B) minus the Lepton number (L) to a fundamental Abelian symmetry group. This origin for the mass of the referenced bosons means model is already very heavily constricted due to long-standing direct searches in the Large Hadron Collide (LHC).

Trough this model we can also address the metastability of the electroweak (EW) vacuum in the SM trough the new scalar. Allowing for Higgs stabilization up to the plank scale with a the new Higgs starting from few hundred of GeVs.

The B-L-SM is particular interesting in the context of the study of Grand Unified Theories (GUT) as it easily embedded into higher order symmetry groups like for example the SO(10) [6, 7, 8, 9, 10] or E_6 [11, 12, 13].

This model includes the presence of a new complex singlet field, χ. This field's interactions with a Higgs doublet typically would result in enhanced strength of the EW phase transition potentially converting it into a strong first-order one, this would be could be detectable in the form of a gravitational wave background. Maybe in a future work section

Such a analysis is of utmost importance given that it could provide a way to detect new physics without the need for a larger particle collider but instead a sensitive probe also capable of studying gravitational events.

However a family-universal symmetry such as $\mathrm{U}(1)_{\mathrm{B-L}}$ being introduced without changing the SM fermion content would lead to chiral anomalies. This translates to a non conservative charged current on some channels involving the $\mathrm{U}(1)_{\mathrm{B-L}}$. These aren't completely undesired by themselves, since their result would be charge conjugation parity symmetry violation, but this inclusion at tree-level without a suppression mechanism would lead to far too much CP violation. is this true ? And why is it true

The model also benefits from presence of three generations of right-handed heavy Majorana neutrinos that trough the new field additions are possible in a framework free of anomalies while also enabling a minimal see-saw mechanism to generate light neutrino masses unlike the SM. [14, 15, 16]. I never mention anomalies, should I go in-depth?

The mass scale of such neutrinos is established once the $\mathrm{U}(1)_{\mathrm{B-L}}$ symmetry is broken by the VEV, x, of the complex singlet scalar field, χ. This VEV simultaneously gives mass to the corresponding Z' boson and H'. These neutrinos are of cosmological significance given their presence could imply the existence of a sterile state that can play the role of Dark Matter candidate [17]. The relatively small alteration of a, $\mathbb{Z}_2$, symmetry in the neutrino sector can make these fully sterile, as seen in [18, 19]. Check if the Z2 affects the Zprime, if so we must comment that it doens't allow kinetic mixing! and would alter the a_μ These neutrinos can, in such case, be used to help explain the baryon asymmetry via the leptogenesis mechanism, this scenario is discussed in depth in the following Refs. [20, 21, 22].

The goal of this chapter is to present the fundamental theoretical background on the model with a strong focus on the basic details of scalar and gauge boson mass spectra and mixing. Followed by a modern precise study of the phenomenological status of the B-L-SM model trough a layered algorithm that will be discussed preceding the results. Through this algorithm we provide a numerical analysis that tests the relevant phenomenological constraints in direct and electroweak observables. Followed by this study we table of a few representative benchmark points to be possibly tested in by experiments.

3.1 Formulating the model

Essentially, the minimal B-L-SM is a Beyond the Standard Model (BSM) framework containing only three new ingredients, a new gauge interaction given the new symmetry group, three generations of right handed neutrinos, and a complex scalar field χ.

The first of these, is motivated by the aforementioned GUT scenarios, as seen in the Refs, [6, 7, 8, 9, 10, 11, 12, 13].

Secondly, as mentioned, a new sector of additional three $U(1)_{B-L}$ charged Majorana neutrinos is essential for anomaly cancellation and addresses many concerns of the SM.

Finally, the SM-like Higgs doublet, H, does not carry neither baryon nor lepton number, this way it does not participate in the breaking of $U(1)_{B-L}$. It is then necessary to introduce a new scalar singlet field, χ, solely charged under $U(1)_{B-L}$, to perform the breaking of the $B-L$ symmetry.

The particle content and related charges of the minimal $U(1)_{B-L}$ extension of the SM are shown in the table. Note these are similar to the SM as to be expected.

	q_L	u_R	d_R	l_L	e_R	ν_R	H	χ
$SU(3)_c$	3	3	3	1	1	1	1	1
$SU(2)_L$	2	1	1	2	1	1	2	1
$U(1)_Y$	$\frac{1}{6}$	$\frac{2}{3}$	$-\frac{1}{3}$	$-\frac{1}{2}$	-1	0	$\frac{1}{2}$	0
$U(1)_{B-L}$	$\frac{1}{3}$	$\frac{1}{3}$	$\frac{1}{3}$	-1	-1	-1	0	2

Table 3.1: Quantum fields and their respective quantum numbers in the minimal B-L-SM extension. The last two lines represent the weak and $B-L$ hypercharges

Scalar sector

Given the information seen above, we can begin examining the new Lagrangian terms. Starting by the scalar potential, which now depends on two fields as seen in,

$$V(H,\chi) = \mu_1^2 H^\dagger H + \mu_2^2 \chi^* \chi + \lambda_1 (H^\dagger H)^2 + \lambda_2 \left(\chi^* \chi\right)^2 + \lambda_3 \chi^* \chi H^\dagger H \tag{3.1}$$

Should I define what these are? Like λ_i scalar couplings and μ terms bla bla bla?. This potential must lead to stable vacuum state, for this the scalar potential must be bounded from below (BFB), as to ensure a global minima. Studying the potential on eq. 3.1 we deduce the conditions,

$$4\lambda_1\lambda_2 - \lambda_3^2 > 0 \quad , \quad \lambda_1, \lambda_2 > 0 \tag{3.2}$$

Where the full components of the scalar fields H and χ are given by,

$$H = \frac{1}{\sqrt{2}} \begin{pmatrix} -i\left(\omega_1 - i\omega_2\right) \\ v + (h + iz) \end{pmatrix} \qquad \chi = \frac{1}{\sqrt{2}}\left(x + (h' + iz')\right) \tag{3.3}$$

In these equations we can see h and h' representing the radial quantum fluctuations around the minimum of the potential. These will constitute the physical degrees of freedom associated to the H and H'. There are also four Goldstone directions denoted as ω_1, ω_2, z and z' which are absorbed into longitudinal modes of the $W^{\pm}$, Z and Z' gauge bosons once spontaneous symmetry breaking (SSB) takes place. After SSB the associated VEVs take the form,

$$\langle H \rangle = \frac{1}{\sqrt{2}} \begin{pmatrix} 0 \\ v \end{pmatrix} \qquad \langle \chi \rangle = \frac{x}{\sqrt{2}} \tag{3.4}$$

From here we can solve the tadpole equations in relation to each of the VEVs as to ensure non-zero minima, we arrive at,

$$v^2 = \frac{-\lambda_2\mu_1^2 + \frac{\lambda_3}{2}\mu_2^2}{\lambda_1\lambda_2 - \frac{1}{4}\lambda_3^2} > 0 \qquad \text{and} \qquad x^2 = \frac{-\lambda_1\mu_2^2 + \frac{\lambda_3}{2}\mu_1^2}{\lambda_1\lambda_2 - \frac{1}{4}\lambda_3^2} > 0 \tag{3.5}$$

which, when simplified with the bound from bellow conditions yield a simpler set of equations,

$$\lambda_2\mu_1^2 < \tfrac{\lambda_3}{2}\mu_2^2 \qquad \text{and} \qquad \lambda_1\mu_2^2 < \tfrac{\lambda_3}{2}\mu_1^2 \tag{3.6}$$

Note that although λ_1 and λ_2 must be positive to ensure the correct conical shape to the potential, no such conditions exist for the sign of λ_3 , μ_1, and μ_2. However observing equation 3.6 we can infer that only some combinations of signs are impossible,

	$\mu_2^2 > 0$ $\mu_1^2 > 0$	$\mu_2^2 > 0$ $\mu_1^2 < 0$	$\mu_2^2 < 0$ $\mu_1^2 > 0$	$\mu_2^2 < 0$ $\mu_1^2 < 0$
$\lambda_3 < 0$	✗	✓	✓	✓
$\lambda_3 > 0$	✗	✗	✗	✓

Table 3.2: Possible Signs of the potential parameters in (3.1). While the ✓ symbol indicates the existence of solutions for tadpole conditions (3.6), the ✗ indicates unstable configurations.

For our numerical analysis we decided to leave the sign of λ_3 positive, choosing a configuration where both μ parameters are negative. This doesn't directly translate to any real physical consequence. These conditions now established we proceed to investigate the physical states of B-L-SM scalar sector. By first, taking the Hessian matrix evaluated at the vacuum value,

$$\mathbf{M}^2 = \begin{pmatrix} 4\lambda_2 x^2 & \lambda_3 v x \\ \lambda_3 v x & 4\lambda_1 v^2 \end{pmatrix}, \tag{3.7}$$

Moving this matrix to it's physical mass eigen-base, we obtain the following eigenvalues,

$$m_{h_{1,2}}^2 = \lambda_1 v^2 + \lambda_2 x^2 \mp \sqrt{(\lambda_1 v^2 - \lambda_2 x^2)^2 + (\lambda_3 x v)^2}\,, \tag{3.8}$$

The physical basis vectors h_1 and h_2 can then be related to the original fields of gauge eigen-basis h and h' trough a simple rotation matrix:

$$\begin{pmatrix} h_1 \\ h_2 \end{pmatrix} = \mathbf{O} \begin{pmatrix} h \\ h' \end{pmatrix}. \tag{3.9}$$

Being that, the rotation matrix is written as,

$$\mathbf{O} = \begin{pmatrix} \cos\alpha_h & -\sin\alpha_h \\ \sin\alpha_h & \cos\alpha_h \end{pmatrix} . \tag{3.10}$$

Recall that due to the SSB order $x > v$. The precise mixing angle is represented simply by,

$$\tan 2\alpha_h = \frac{|\lambda_3|\, vv'}{\lambda_1 v^2 - \lambda_2 v'^{\,2}} \tag{3.11}$$

Although consider it is worth presenting the case of approximate decoupling where, $v/x \ll 1$. In this case scalar masses and mixing angle become particularly simple,

$$\sin\alpha_h \approx \frac{1}{2}\frac{\lambda_3}{\lambda_2}\frac{v}{x} \qquad m_{h_1}^2 \approx 2\lambda_1 v^2 \qquad m_{h_2}^2 \approx 2\lambda_2 x^2 \tag{3.12}$$

We will see in the context of our numerical results that for our phenomenologically consistent mass scale these equations serve a valid approximation for most of the points.

Gauge Sector

Moving onto the gauge boson and Higgs kinetic terms in the B-L-SM, consider the following portion of the Lagrangian,

$$\mathcal{L}_{U(1)'s} = |D_\mu H|^2 + |D_\mu \chi|^2 - \frac{1}{4}F_{\mu\nu}F^{\mu\nu} - \frac{1}{4}F'_{\mu\nu}F'^{\mu\nu} - \frac{1}{2}\kappa F_{\mu\nu}F'^{\mu\nu} \tag{3.13}$$

where $F^{\mu\nu}$ and $F'^{\mu\nu}$ are the standard field strength tensors, respectively for the hypercharge $\mathrm{U(1)_Y}$ and B minus L $\mathrm{U(1)_{B-L}}$,

$$F_{\mu\nu} = \partial_\mu A_\nu - \partial_\nu A_\mu \qquad \text{and} \qquad F'_{\mu\nu} = \partial_\mu A'_\nu - \partial_\nu A'_\mu \, . \tag{3.14}$$

written in terms of the gauge fields A_μ and A'_μ, respectively. Given that this is a model with two Unitary groups, without a parity symmetry ($\mathbb{Z}_2$) to prevent it, we must consider the possible mixing in between them. In this work we parametrized this mixing trough a parameter κ.

The Abelian part of the covariant derivative in equation 3.13 is given by,

$$D_\mu \supset i g_1 Y A_\mu + i g'_1 Y_{\mathrm{B-L}} A'_\mu \, , \tag{3.15}$$

with g_1 and g'_1 being the $\mathrm{U(1)_Y}$ and $\mathrm{U(1)_{B-L}}$ the gauge couplings with the Y and $B-L$ charges are specified in Tab. 3.1. However it is convenient to rewrite the gauge kinetic terms in the canonical form, i.e.

$$F_{\mu\nu}F^{\mu\nu} + F'_{\mu\nu}F'^{\mu\nu} + 2\kappa F_{\mu\nu}F'^{\mu\nu} \to B_{\mu\nu}B^{\mu\nu} + B'_{\mu\nu}B'^{\mu\nu} \, . \tag{3.16}$$

A generic orthogonal transformation in the field space does not eliminate the kinetic mixing term. So, in order to satisfy Eq. (3.16) an extra non-orthogonal transformation should be imposed such that Eq. (3.16) is realized. Taking $\kappa = \sin\alpha$, a suitable redefinition of fields $\{A_\mu, A'_\mu\}$ into $\{B_\mu, B'_\mu\}$ that eliminates κ-term according to Eq. (3.13) can be cast as

$$\begin{pmatrix} A_\mu \\ A'_\mu \end{pmatrix} = \begin{pmatrix} 1 & -\tan\alpha \\ 0 & \sec\alpha \end{pmatrix} \begin{pmatrix} B_\mu \\ B'_\mu \end{pmatrix} , \tag{3.17}$$

Note there is a limit without kinetic mixing where $\alpha = 0$. Note that this transformation is generic and valid for any basis in the field space. The transformation (3.17) results in a modification of the covariant derivative that acquires two additional terms encoding the details of the kinetic mixing, i.e.

$$D_\mu \supset \partial_\mu + i\,(g_Y\, Y + g_B Y\, Y_{B-L})\, B_\mu + i\,(g_{B-L}\, Y_{B-L} + g_{YB}\, Y)\, B'_\mu \, , \tag{3.18}$$

where the gauge couplings take the form

$$\begin{cases} g_Y = g_1 \\ g_{B-L} = g_1' \sec\alpha \\ g_{YB} = -g_1 \tan\alpha \\ g_{BY} = 0 \end{cases}, \tag{3.19}$$

which is the standard convention in the literature. Note this definition is merely to simply the equations and has no physical impact. We will later see that this kinetic mixing is a desired feature and why stabilizing it with a $\mathbb{Z}_{\not\in}$ symmetry would be detrimental in terms of depth. The resulting mixing between the neutral gauge fields including Z' can be represented as follows

$$\begin{pmatrix} \gamma_\mu \\ Z_\mu \\ Z'_\mu \end{pmatrix} = \begin{pmatrix} \cos\theta_W & \sin\theta_W & 0 \\ -\sin\theta_W\cos\theta'_W & \cos\theta_W\cos\theta'_W & \sin\theta'_W \\ \sin\theta_W\sin\theta'_W & -\cos\theta'_W\sin\theta'_W & \cos\theta'_W \end{pmatrix} \begin{pmatrix} B_\mu \\ A^3_\mu \\ B'_\mu \end{pmatrix} \tag{3.20}$$

where θ_W is the weak mixing angle and θ'_W is defined as

$$\sin(2\theta'_W) = \frac{2g_{YB}\sqrt{g^2+g_Y^2}}{\sqrt{(g_{YB}^2 + 16(\frac{x}{v})^2 g_{B-L}^2 - g^2 - g_Y^2)^2 + 4g_{YB}^2(g^2+g_Y^2)}}\,, \tag{3.21}$$

in terms of g and g_Y being the $SU(2)_L$ and U_Y gauge couplings, respectively. In the physically relevant limit, $v/x \ll 1$, the above expression greatly simplifies leading to

$$\sin\theta'_W \approx \frac{1}{16}\frac{g_{YB}}{g_{B-L}}\left(\frac{v}{x}\right)^2\sqrt{g^2+g_Y^2}\,, \tag{3.22}$$

up to $(v/x)^3$ corrections. In the limit of no kinetic mixing, i.e. $g_{YB} \to 0$, there is no mixture of Z' and SM gauge bosons.

Note, the kinetic mixing parameter θ'_W has rather stringent constraints from Z pole experiments both at the Large Electron-Positron Collider (LEP) and the Stanford Linear Collider (SLC), restricting its value to be smaller than 10^{-3} approximately, which we set as an upper bound in our numerical analysis. Expanding the kinetic terms $|D_\mu H|^2 + |D_\mu \chi|^2$ around the vacuum one can extract the following mass matrix for vector bosons

$$m_V^2 = \frac{v^2}{4}\begin{pmatrix} g^2 & 0 & 0 & 0 & 0 \\ 0 & g^2 & 0 & 0 & 0 \\ 0 & 0 & g^2 & -gg_Y & -gg_{YB} \\ 0 & 0 & -gg_Y & g_Y^2 & g_Y g_{YB} \\ 0 & 0 & -gg_{YB} & g_Y g_{YB} & g_{YB}^2 + 16\left(\frac{x}{v}\right)^2 g_{B-L}^2 \end{pmatrix} \tag{3.23}$$

whose, first set eigenvalues read,

$$m_A = 0\,, \qquad m_W = \tfrac{1}{2}vg \tag{3.24}$$

corresponding to the expected physical photon and $W^\pm$ bosons. While the following set,

$$m_{Z,Z'} = \sqrt{g^2+g_Y^2}\cdot\frac{v}{2}\sqrt{\frac{1}{2}\left(\frac{g_{YB}^2 + 16(\frac{x}{v})^2 g_{\mathrm{BL}}^2}{g^2+g_Y^2}+1\right) \mp \frac{g_{YB}}{\sin(2\theta'_W)\sqrt{g^2+g_Y^2}}}\,. \tag{3.25}$$

correspond to two neutral massive vector bosons, with one of them, not necessarily the lightest, representing the SM-like Z boson. It follows from LEP and SLC constraints on θ'_W, that Eq. (3.22) also implies that either g_{YB} or the ratio $\frac{v}{x}$ are small. In this limit, Eq. (3.25) simplifies to

$$m_Z \approx \tfrac{1}{2}v\sqrt{g^2+g_Y^2} \qquad \text{and} \qquad m_{Z'} \approx 2g_{B-L}x\,, \tag{3.26}$$

where the $m_{Z'}$ depends only on the SM-singlet VEV ,x and on the $\mathrm{U(1)_{B-L}}$ gauge coupling and will be attributed to a heavy Z' state, while the light Z-boson mass corresponds to its SM value.

The Yukawa sector

One of the key features of the B-L-SM is the presence of non-zero neutrino masses. In its minimal version, such masses are generated via a type-I seesaw mechanism, thus producing a very light neutrino for each of the three known neutrino flavours, and a corresponding very heavy neutrino for each, which has yet to be observed. In the type-I seesaw mechanism the mixing of neutrinos fields is written with similar shape to,

$$\begin{pmatrix} 0 & A \\ A & B \end{pmatrix} \tag{3.27}$$

This system would have a set eigenvalues written as,

$$\lambda_{\pm} = \frac{B \pm \sqrt{B^2 + 4A}}{2} \tag{3.28}$$

Investigating the nature of this set of eigenvalues allows us to understand the see-saw. The mean of these values being always equal to $|B|$, if one value goes up, another goes down, like a see-saw. Note B, generally is the Majorana mass terms, and is generally very large in comparison to the cross interaction terms. Given this the smaller eigenstate to be approximate,

$$\lambda_{-} \approx \frac{A^2}{B} \tag{3.29}$$

This mechanism serves to explain why the neutrino masses are so small.

The total Yukawa Lagrangian of the model reads,

$$\mathcal{L}_f = -Y_u^{ij}\overline{q_{\mathrm{Li}}}u_{\mathrm{Rj}}\widetilde{H} - Y_d^{ij}\overline{q_{\mathrm{Li}}}d_{\mathrm{Rj}}H - Y_e^{ij}\overline{\ell_{\mathrm{Li}}}e_{\mathrm{Rj}}H - Y_\nu^{ij}\overline{\ell_{\mathrm{Li}}}\nu_{\mathrm{Rj}}\widetilde{H} - \frac{1}{2}Y_\chi^{ij}\overline{\nu^c_{\mathrm{Ri}}}\nu_{\mathrm{Rj}}\chi + \mathrm{c.c.} \tag{3.30}$$

Notice the explicit lack of Majorana neutrino mass terms of the form $M\overline{\nu^c_R}\nu_R$. These explicitly violate the $\mathrm{U}(1)_{\mathrm{B-L}}$ symmetry and are therefore not present. In Eq. (3.30), Y_u, Y_d and Y_e are the 3×3 Yukawa matrices that reproduce the quark and charged lepton sector exactly the same way as in the SM, while Y_ν and Y_χ are the new Yukawa matrices responsible for the generation of right handed neutrino masses and mixing with left handed fields. In particular, one can write,

$$\mathbf{m}_{\nu_l}^{Type-I} = \frac{1}{\sqrt{2}}\frac{v^2}{x}\mathbf{Y}_\nu^t \mathbf{Y}_\chi^{-1}\mathbf{Y}_\nu\,, \tag{3.31}$$

for light ν_l neutrino masses, whereas the heavy ν_h ones are given by

$$\mathbf{m}_{\nu_h}^{Type-I} \approx \frac{1}{\sqrt{2}}\mathbf{Y}_\chi x\,, \tag{3.32}$$

where we have assumed a flavour diagonal basis.

Note that the smallness of light neutrino masses imply that either the x VEV is very large or (if we fix it to be at the $\mathcal{O}(TeV)$ scale and $\mathbf{Y}_\chi \sim \mathcal{O}(1)$) the corresponding Yukawa coupling should be tiny, $\mathbf{Y}_\nu < 10^{-6}$. It is clear that the low scale character of the type-I seesaw mechanism in the minimal B-L-SM is *faked* by small Yukawa couplings to the Higgs boson. A more elegant description was proposed in Ref. [23] where small SM neutrino masses naturally result from an inverse seesaw mechanism. In this work, however, we will not study the neutrino sector and thus, for an improved efficiency of our numerical analysis of Z' observables, it will be sufficient to fix the Yukawa couplings to $\mathbf{Y}_\chi = 10^{-1}$ and $\mathbf{Y}_\nu = 10^{-7}$ values such that the three lightest neutrinos lie in the sub-eV domain.

I think I should show more of the diagonalization process? This last part seems barren

3.2 Numerical Results

Perhaps a small introduction

Before we begin this section consider that our colleges in a recent work tested the state of the art at the LHC for low mass Z' boson. In particular from 0.2GeV to 200GeV. As for slightly heavier Z' masses beyond $m_{Z'} \gtrsim 100$ GeV, the combined effect of the electroweak precision observables and the ATLAS searches for Drell-Yan Z' production decaying into di-leptons, i.e. $pp \to Z' \to ee, \mu\mu$ [1], is also finely investigated.

We then endeavoured to achieve a complementary study where we investigated the case of very heavy Z' bosons. Our goal can be summarized as, discover if it was possible to, with such a heavy Z' boson, limited by LHC, with such a heavily constrained kinetic mixing, to have any significant phenomenological impact asides from simply a yet to be observed boson. This was chiefly done by the investigation of the $(g-2)_\mu$ anomaly.

We examine the relations that this anomaly has with the paramater space, such as gauge couplings, as well as the extra scalar mass. The $(g-2)_\mu$ anomaly refers to the discrepancy between the measured anomalous magnetic moment of the muon, $a_\mu^{\rm exp} \equiv \frac{1}{2}g - 2)_\mu^{\rm exp}$, and its theoretical prediction, $a_\mu^{\rm SM} \equiv \frac{1}{2}(g-2)_\mu^{\rm SM}$, which reads [5]

$$\Delta a_\mu = a_\mu^{\rm exp} - a_\mu^{\rm SM} = 268(63)(43) \times 10^{-11} \tag{3.33}$$

with numbers in brackets denoting experimental and theoretical errors, respectively. This represents a tension of 3.5 standard deviations from the combined 1σ error and is calling for new physics effects beyond the SM theory. A popular explanation for such an anomaly resides in low-scale supersymmetric models [**?**, **?**, **?**, **?**, **?**, **?**, **?**, **?**, **?**, **?**, **?**] where smuon-neutralino and sneutrino-chargino loops can explain the discrepancy (3.33). However, this solution is by no means unique and radiative corrections with new gauge bosons can also enhance the theoretical value of the muon anomaly such that (3.33) is satisfied [**?**]. This is indeed the case of the B-L-SM, or its SUSY version [**?**, **?**], where a new Z' gauge boson can explain Δa_μ.

Scanning tools and parameter space bounds

The numerical data presented in this section was generated thorough a large chain of layered scripts that were created as a possible first generation for a scanning apparatus for phenomenological models. We will this was later adapted and translated to the 3HDM numerical scans. The scripts were a mixture of Linux bash and Python 3 scripts. These scripts Generate a Monte-Carlo type scan through a desired parameter space. All couplings and physical constants are generated and their spectrum calculated before a second layer checks said spectrum against a large number of constraints. Our scanning routine randomly samples parameter space points according to the ranges in Tab. 3.3. Keeping the remaining free parameters of the model to be in agreement with

λ_1	$\lambda_{2,3}$	$g_{\rm B-L}$	$g_{\rm YB}$	x [TeV]
$[10^{-2},\ 10^{0.5}]$	$[10^{-8},\ 10]$	$[10^{-8},\ 10]$	$[10^{-8},\ 10]$	$[0.5,\ 20.5]$

Table 3.3: Parameter scan ranges used in our analysis. Note that the value of λ_1 is mostly constrained by the tree-level Higgs boson mass given in Eq. (3.12).

the Standard Model.

The checks applied were sequential and begin with the "zero-th" check where our spectrum generator `SPheno`, promptly rejects any scenario with tachyonic scalar masses and un-renormalizable quantities.

`SPheno` is a particle spectrum generator code written in Fortran 90. It's emphasis on easy generalisability and speed made it a natural part of our numerical analysis. It takes information about our models Lagrangian, such as fields, charges and fundamental symmetries, and creates a executable file capable of quickly generating a spectrum file with all details regarding mass, decay and flavour observables information in the standardized SUSY Les-Houches accord format. All generated spectrums are processed and stored. This Lagrangian information is fed to `SPheno` also in standardized format automatically generated by a Mathematica packaged designed for such purposes called `SARAH`.

All points that complete this zero-th layer, have their information regarding two and three body decays, in particular to the Higgs bosons, passed along to another set Fortran 90 packages called `HiggsBounds` and `HiggsSignals`. These test experimental detection limits for the new scalars and verify if we have a "SM" like Higgs to account for the detected boson.

Parameter Space

However the presence of new bosons in the theory can lead to large deviations in EW precision observables. Typically, the most stringent constraints of the scalar sector emerge from the oblique S, T, U parameters, which are also calculated by `SPheno`. Current precision measurements provide the allowed regions,

$$S = 0.02 \pm 0.10\,, \qquad T = 0.07 \pm 0.12\,, \qquad U = 0.00 \pm 0.09 \tag{3.34}$$

where S-T are 92% correlated, while S-U and T-U are -66% and -86% anti-correlated, respectively. We compare our results with the EW fit in Eq. (3.34) and require consistency with the best fit point within a 95% C.L. ellipsoid (see Ref. [24] for further details about this method). We show in Fig. 4.5 our results in the ST (left) and TU (right) planes where black points are consistent with EW precision observables at 95% C.L. whereas grey ones lie outside the corresponding ellipsoid of the best fit point and, thus, are excluded in our analysis.

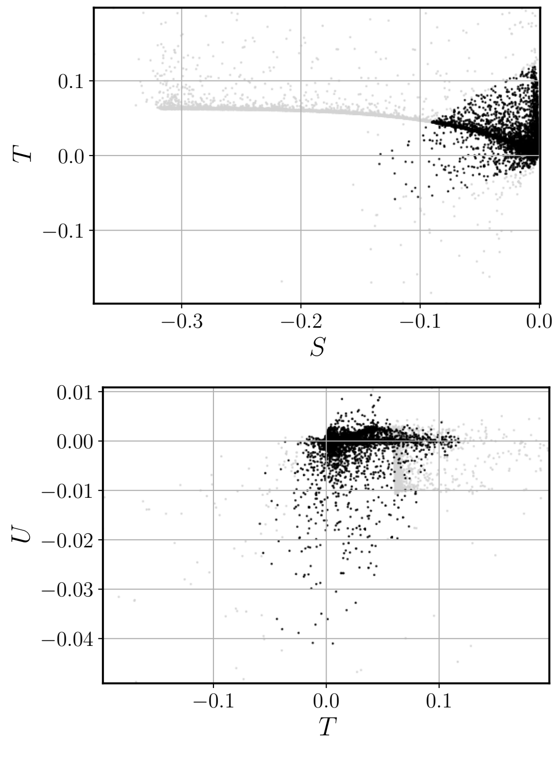

Figure 3.1: Scatter plots for EW precision observables showing the ST (left) and TU (right) planes. Accepted points lying within a 95% C.L. ellipsoid of the best fit point are represented in black whereas grey points are excluded.

Thus, in a second layer of phenomenological tests, we confront the surviving scenarios, black points in Fig. 4.5, with collider bounds. In particular, we use `HiggsBounds 4.3.1` [25] to apply 95% C.L. exclusion limits on a new scalar particle, h_2, and `HiggsSignals 1.4.0` [26] to check for consistency with the observed Higgs boson taking into account all known Higgs signal data. For the latter, we have accepted points whose fit to the data replicates the observed signal at 95% C.L. while the measured value for its mass, $m_{h_1} = 125.10 \pm 0.14$ GeV [5], is reproduced within a 3σ uncertainty. The required input data for `HiggsBounds/HiggsSignals` are generated by the `SPheno` output in the format of a SUSY Les Houches Accord (SLHA) [27] file. In particular, it provides scalar masses, total decay widths, Higgs decay branching ratios as well as the SM-normalized effective Higgs couplings to fermions and bosons squared (that are needed for analysis of the Higgs boson production cross sections). For details about this calculation, see Ref. [25].

On a third layer of phenomenological tests we have studied the viability of the surviving scenarios from the perspective of direct collider searches for a new Z' gauge boson. We have used `MadGraph5_aMC@NLO 2.6.2` [28] to compute the Z' Drell-Yan production cross section and subsequent decay into the first and second-generation leptons, i.e. $\sigma\,(pp \to Z') \times B\,(Z' \to \ell\ell)$ with $\ell = e,\ \mu$, and then compared our results to the most recent ATLAS exclusion bounds from the LHC runs at the center-of-mass energy $\sqrt{s} = 13$ TeV [1]. The `SPheno` SLHA output files were used as parameter cards for `MadGraph5_aMC@NLO`, where the information required to calculate $\sigma\,(pp \to Z') \times B\,(Z' \to \ell\ell()$, such as the Z' boson mass, its total width and decay branching ratios into lepton pairs, is provided.

The lepton anomalous magnetic moments $(g-2)_\ell/2 \equiv a_\ell$ are calculated in `SPheno` at one-loop order. In the B-L-SM, new physics (NP) contributions to a_μ, denoted as $\Delta a_\mu^{\mathrm{NP}}$ in what follows, can emerge from the diagrams containing Z' or h_2 propagators.

Discussion of numerical results

Let us now discuss the phenomenological properties of the B-L-SM model. First, we focus on the current collider constraints and study their impact on both the scalar and gauge sectors.

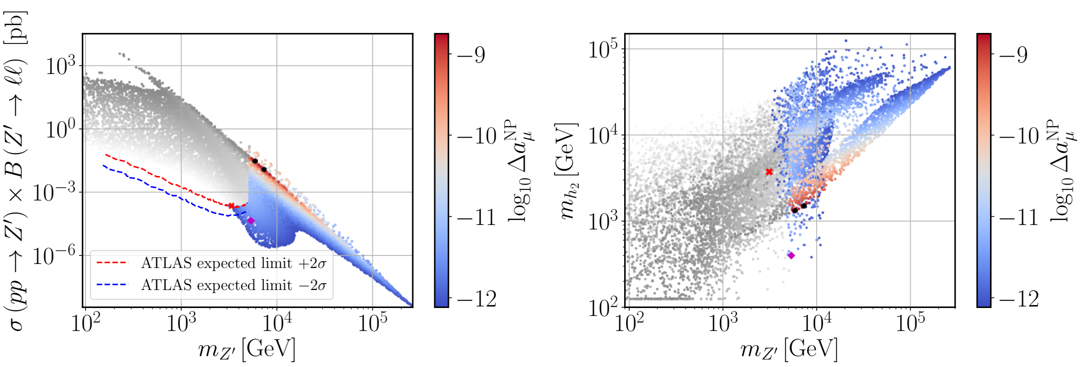

Figure 3.2: Scatter plots showing the Z' Drell-Yan production cross section times the decay branching ratio into a pair of electrons and muons (left panel) and the new scalar mass m_{h_2} (right panel) as functions of $m_{Z'}$ and the new physics (NP) contributions to the muon Δa_μ anomaly. Coloured points have survived all theoretical and experimental constraints while grey points are excluded by direct Z' searches at the LHC. The region between the two dashed lines represents the current ATLAS expected limit on the production cross section times branching ratio into a pair of leptons at 95% C.L. and is taken from the *Brazilian* plot in Fig. 4 of Ref. [1]. The four highlighted points in both panels denote the benchmark scenarios described in detail in Tab. 3.4.

We show in Fig. 3.2 the scenarios generated in our parameter space scan (see Tab. 3.3) that have passed all theoretical constraints such as boundedness from below, unitarity and EW precision tests, are compatible with the SM Higgs data and where a new visible scalar h_2 is unconstrained by the direct collider searches. On the left panel, we show the Z' production cross section times its branching ratio to the first- and second-generation leptons, $\sigma B \equiv \sigma\left(pp \to Z'\right) \times B\left(Z' \to \ell\ell\right)$ with $\ell = e, \mu$, as a function of the new vector boson mass and the new physics contribution to the muon anomalous magnetic moment $\Delta a_\mu^{\mathrm{NP}}$ (colour scale). On the right panel, we show the new scalar mass as a function of the same observables. All points above the red dashed line are excluded at 95% C.L. by the upper expected limit on Z' direct searches at the LHC by the ATLAS experiment and are represented in grey shades. Darker shades denote *would-be-scenarios* with larger values of $\Delta a_\mu^{\mathrm{NP}}$ while the smaller contributions to the muon $(g-2)_\mu/2$ anomaly are represented with the lighter shades. The region between the two dashed lines corresponds to the Z' ATLAS limit with a 2σ uncertainty represented by the yellow band in Fig. 4 of [1]. Provided that the observed limit by the ATLAS detector lies within this region we have taken a conservative approach and accepted all points whose σB value lies below the red dashed line (upper limit) in Fig. 3.2. The blue dashed line, which corresponds to the stricter 2σ lower bound, is only shown for completeness of information. The red cross in our figures signals the lightest Z' found in our scan which we regard as a possible early-discovery (or early-exclusion) benchmark point in the forthcoming LHC runs. Such a benchmark point is shown in the first line of Tab. 3.4. On the right panel, we notice that the new scalar bosons can become as light as $380-400$ GeV, but with Z' masses in the range of $5-9$ TeV. We highlight with a magenta diamond the benchmark point with the lightest Z' boson within this range. This point is shown in the second line of Tab. 3.4.

$m_{Z'}$	m_{h_2}	x	$\log_{10}\Delta a_\mu^{\mathrm{NP}}$	σB	θ'_W	α_h	$g_{\text{B-L}} \simeq g^{\ell\ell Z'}$
3.13	3.72	15.7	-12.1	2.22×10^{-4}	≈ 0	5.67×10^{-5}	0.0976
5.37	0.396	9.10	-11.7	4.23×10^{-5}	2.55×10^{-7}	9.44×10^{-7}	0.302
7.35	1.49	0.321	-8.75	0.0115	1.83×10^{-7}	1.20×10^{-6}	3.15
5.91	1.32	0.335	-8.78	0.0285	1.30×10^{-4}	1.04×10^{-5}	2.94

Table 3.4: A selection of four benchmark points represented in Figs. 3.2, 3.4 to 3.6. The $m_{Z'}$, m_{h_2} and x parameters are given in TeV. The first line represents a point with light h_2 while the second line shows the lightest allowed Z' boson found in our scan. The last two lines show two points that reproduce the observed value of the muon $(g-2)$ within 1σ uncertainty.

Implications of direct Z' searches at the LHC for the $(g-2)_\mu$ anomaly

Looking again to Fig. 3.2 (left panel), we see that there is a thin dark-red stripe where $\Delta a_\mu^{\mathrm{NP}}$ explains the observed anomaly shown in Eq. (3.33) for a range of $m_{Z'}$ boson masses approximately between 5 TeV and 20 TeV. This region is particularly interesting as it can be partially probed by the forthcoming LHC runs or at future colliders. If a Z' boson discovery remains elusive for such a mass range, it can exclude a possibility of explaining the muon $(g-2)_\mu$ anomaly in the context of the B-L-SM. It is also worth noticing that such preferred $\Delta a_\mu^{\mathrm{NP}}$ values represent a small island in the right plot of Fig. 3.2 where the new scalar boson mass is restricted to the range of 1 TeV $< m_{h_2} <$ 4 TeV.

New physics contributions $\Delta a_\mu^{\mathrm{NP}}$ to the muon anomalous magnetic moment are given at one-loop order by the Feynman diagrams depicted in Fig. 3.3. Since the couplings of a new scalar h_2 to the SM fermions are suppressed by a factor of $\sin\alpha_h$, which we find to be always smaller than 0.08 as can be seen in the bottom panel of Fig. 3.4, the right diagram in Fig. 3.3, which scales as $\Delta a_\mu^{h_2} \propto \frac{m_\mu^2}{m_{h_2}^2}\left(y_\mu \sin\alpha_h\right)^2$ with $\sin^2\alpha_h < 0.0064$ and $y_\mu = Y_e^{22}$, provides sub-leading contributions to Δa_μ. Furthermore, as we show in the top-left panel of Fig. 3.4 the new scalar boson mass, which we have found to satisfy $m_{h_2} \gtrsim 380$ GeV, is not light enough to compensate the smallness of the scalar mixing angle. Conversely, and recalling that all fermions in the B-L-SM transform non-trivially under $\mathrm{U}(1)_{\mathrm{B-L}}$, the new Z' boson can have sizeable couplings to fermions via gauge interactions proportional to $g_{\mathrm{B-L}}$. Therefore, the left diagram in Fig. 3.3 provides the leading

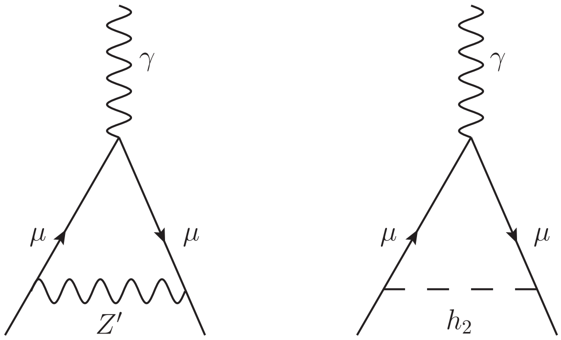

Figure 3.3: One-loop diagrams contributing to $\Delta a_\mu^{\rm NP}$ in the B-L-SM.

contribution to the $(g-2)_\mu$ in the model under consideration. In particular, $\Delta a_\mu^{Z'}$ is given by [29]

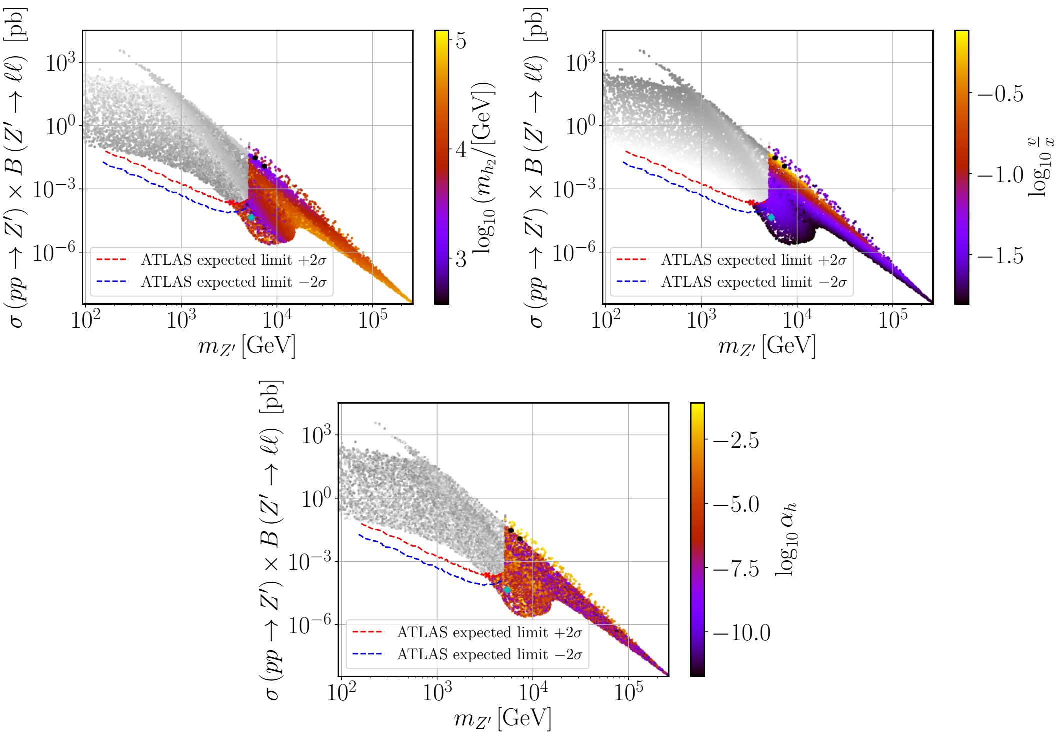

Figure 3.4: Scatter plots showing the Z' Drell-Yan production cross section times the decay branching ratio into a pair of electrons and muons in terms of the $m_{Z'}$ boson mass. The colour gradation represents the new scalar mass (top-left), the ratio between the EW- and $\mathrm{U}(1)_{\mathrm{B-L}}$-breaking VEVs (top-right) and the scalar mixing angle (bottom). The grey points are excluded by direct Z' searches at the LHC. The four benchmark points in Tab. 3.4 are represented by the black dots (last two rows), cyan diamond (first row) and red cross (second row).

$$\Delta a_\mu^{Z'} = \tfrac{1}{12\pi^2}\tfrac{m_\mu^2}{m_{Z'}^2}\left(3g_{\rm L}^{\mu\mu Z'}g_{\rm R}^{\mu\mu Z'} - {g_{\rm L}^{\mu\mu Z'}}^2 - {g_{\rm R}^{\mu\mu Z'}}^2\right) \tag{3.35}$$

where the left- and right-chiral projections of the charged lepton couplings to the Z' boson, $g_{\rm L}^{\ell\ell Z'}$

and $g_{\mathrm{R}}^{\ell\ell Z'}$, respectively, can be approximated as follows

$$\begin{aligned} g_{\mathrm{L}}^{\ell\ell Z'} &\simeq g_{\mathrm{B-L}} + \tfrac{1}{32}\left(\tfrac{v}{x}\right)^2 \tfrac{g_{\mathrm{YB}}}{g_{\mathrm{B-L}}}\left[g_{\mathrm{Y}}^2 - g^2 + 2 g_{\mathrm{Y}} g_{\mathrm{YB}}\right] , \\ g_{\mathrm{R}}^{\ell\ell Z'} &\simeq g_{\mathrm{B-L}} + \tfrac{1}{16}\left(\tfrac{v}{x}\right)^2 \tfrac{g_{\mathrm{YB}}}{g_{\mathrm{B-L}}}\left[g_{\mathrm{Y}}^2 + g_{\mathrm{Y}} g_{\mathrm{YB}}\right] , \end{aligned} \tag{3.36}$$

to the second order in v/x-expansion. If $v/x \ll 1$, corresponding to the darker shades of the color scale in the top-right panel of Fig. 3.4, we can further approximate

$$g_{\mathrm{L}}^{\ell\ell Z'} \simeq g_{\mathrm{R}}^{\ell\ell Z'} \simeq g_{\text{B-L}} \, , \tag{3.37}$$

such that the muon anomalous magnetic moment gets significantly simplified to

$$\Delta a_\mu^{Z'} \simeq \frac{g_{\text{B-L}}^2}{12\pi^2} \frac{m_\mu^2}{m_{Z'}^2} \, . \tag{3.38}$$

Similarly, for the yellow band, which corresponds to the region where $\Delta a_\mu^{\mathrm{NP}}$ is maximized (see top-left panel of Fig. 3.2), a large value of the $\mathrm{U}(1)_{\mathrm{B-L}}$ gauge coupling also allows one to simplify Eq. (3.35) reducing it to the form of Eq. (3.38). This is in fact what we have observed and, for the yellow band region, we see in the bottom panel of Fig. 3.5 that $g_{\text{B-L}} \simeq 3$. A sizeable value of $g_{\text{B-L}}$ is indeed what is contributing to the enhancement of $\Delta a_\mu^{\mathrm{NP}}$, in particular, for the red region in both panels of Fig. 3.2. We show in the third and fourth lines of Tab. 3.4 the two benchmark points that better reproduce the muon anomalous magnetic moment represented by two black dots in Figs. 3.2, 3.4 to 3.6.

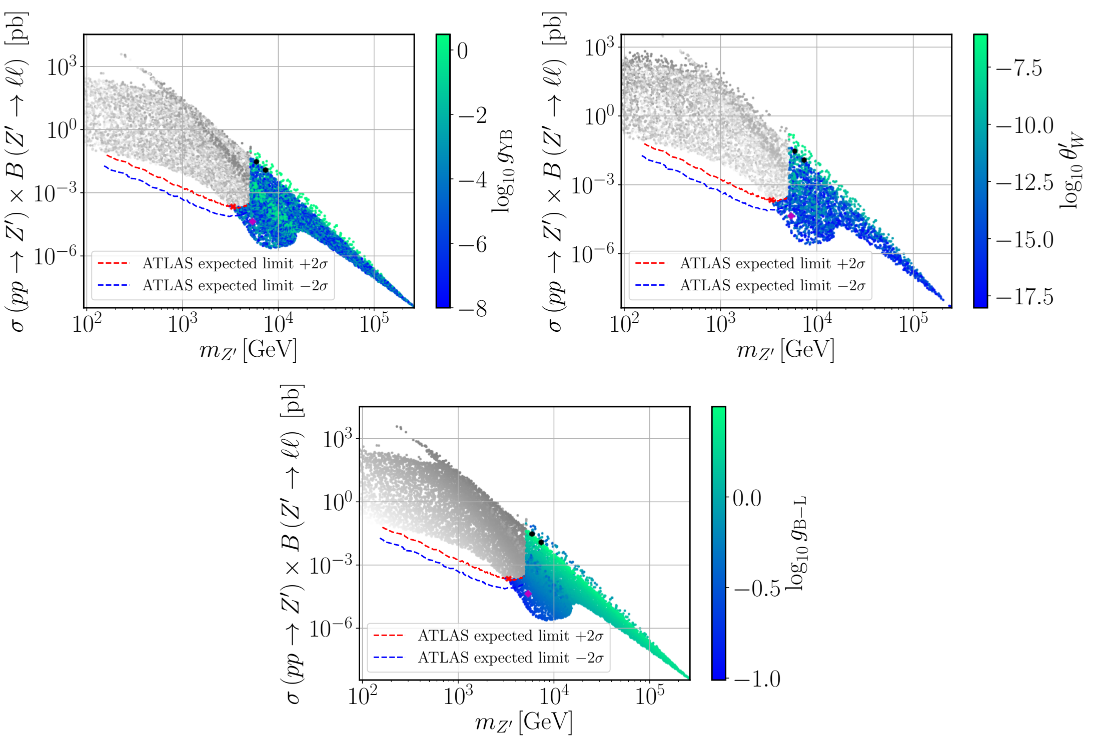

Figure 3.5: The same as in Fig. 3.4 but with the colour scale representing the gauge-mixing parameters g_{YB} (top-left) and θ'_W (top-right), and the $\mathrm{U}(1)_{\mathrm{B-L}}$ gauge coupling (bottom).

In fact, a close inspection of Fig. 3.2 (left panel) and Fig. 3.4 (top-right panel) reveals an almost one-to-one correspondence between the colour shades. This suggests that $\Delta a_\mu^{Z'}$ must somehow be related to the VEV ratio v/x. To understand this behaviour, let us also look to Fig. 3.5 (top-right panel) where we see that the kinetic-mixing gauge coupling $g_{\rm YB}$ is typically very small apart from two green bands where it can become of order $\mathcal{O}(1)$. Interestingly, whenever $g_{\rm YB}$ becomes sizeable, $v/x \ll 1$ is realised, which means that Eq. (3.26) is indeed a good approximation as was argued above. It is then possible to eliminate $g_{\text{B-L}}$ from Eq. (3.38) and rewrite it as

$$\Delta a_\mu^{Z'} \simeq \frac{y_\mu^2}{96\pi^2}\left(\frac{v}{x}\right)^2 , \tag{3.39}$$

which explains the observed correlation between both Fig. 3.2 (left panel) and Fig. 3.4 (top-right panel) and, for instance, the thin red stripe of points compatible with a full description of the muon $(g-2)_\mu/2$ anomaly. Note that this simple and illuminating relation becomes valid as a consequence of the heavy Z' mass regime, in combination with the smallness of the θ'_W mixing angle required by LEP constraints. Indeed, while we have not imposed any strong restriction on the input parameters of our scan (see Tab. 3.3), Eq. (3.22) necessarily implies that both $g_{\rm YB}$ and v/x cannot be simultaneously sizeable in agreement with what is seen in Fig. 3.5 (top-left panel) and Fig. 3.4 (top-right panel). The values of θ'_W obtained in our scan are shown in the top-right panel of Fig. 3.5.

For completeness, we show in Fig. 3.6 the physical couplings of Z' to muons (top panels) and to $W^\pm$ bosons (bottom panel). Note that, for the considered scenarios, the latter can be written

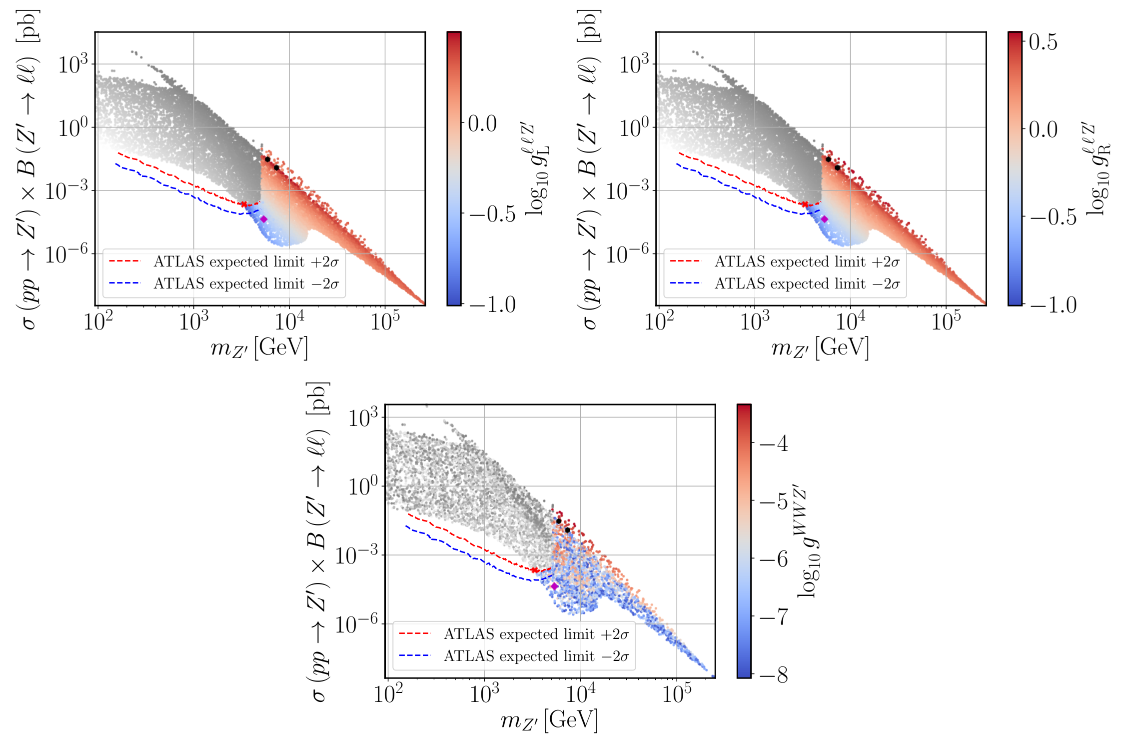

Figure 3.6: The same as in Fig. 3.4 but with the colour scale representing the coupling of leptons to the Z' (top panels) and the coupling of W bosons to Z'.

as

$$g^{WWZ'} \simeq \frac{1}{16}\frac{g_{\rm YB}}{g_{\text{B-L}}}\left(\frac{v}{x}\right)^2 . \tag{3.40}$$

While both $g_{\text{B-L}}$ and the ratio v/x provide a smooth continuous contribution in the $\sigma B - m_{Z'}$ projection of the parameter space, the observed blurry region in $g^{WWZ'}$ is correlated with the one in the top-left panel of Fig. 3.5 as expected from Eq. (3.40). On the other hand, the couplings to leptons $g_{\rm L,R}^{\ell\ell Z'}$ exhibit a strong correlation with $g_{\text{B-L}}$ in Fig. 3.5, in agreement with our discussion above and with Eq. (3.37).

Barr-Zee type contributions

To conclude our analysis, one should note that the two-loop Barr-Zee type diagrams [30] are always sub-dominant in our case. To see this, let us consider the four diagrams shown in Fig. 3.7. The same reason that suppresses the one-loop h_2 contribution in Fig. 3.3 is also responsible

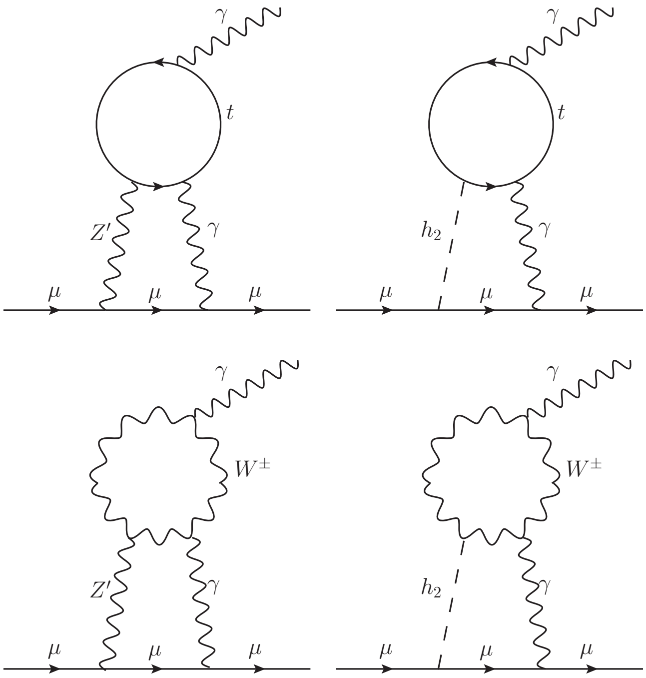

Figure 3.7: Barr-Zee type two-loop diagrams contributing to Δa_μ.

for the suppression of both the top-right and bottom-right diagrams in Fig. 3.7 (for details see e.g. Ref. [31]). Recall that the coupling of h_2 to the SM particles is proportional to the scalar mixing angle α_h, which is always small (or very small) as we can see in Fig. 3.4. An analogous effect is present in the diagram involving a W-loop, where a vertex proportional to $g^{WWZ'}$ suppresses such a contribution. The only diagram that might play a sizeable role is the top-left one where the couplings of Z' to both muons and top quarks are not negligible.

Let us then estimate the size of the first diagram in Fig. 3.7. This type of diagrams were already calculated in Ref. [32] but for the case of a SM Z-boson. Since the same topology holds for the considered case of B-L-SM too, if we trade Z by the new Z' boson, the contribution to the muon $(g-2)_\mu$ anomaly can be rewritten as

$$\Delta a_\mu^{\gamma Z'} = -\frac{g^2 g_{\text{B-L}}^2 m_\mu^2 \tan^2\theta_W}{1536\pi^4}\left(g_{\mathrm{L}}^{ttZ'} - g_{\mathrm{R}}^{ttZ'}\right) \mathrm{T}_7\left(m_{Z'}^2, m_t^2, m_t^2\right) \,, \tag{3.41}$$

where $g_{\mathrm{L,R}}^{ttZ'}$, calculated in `SARAH`, are the left- and right-chirality projections of the Z' coupling to top-quarks, given by

$$\begin{aligned} g_{\mathrm{L}}^{ttZ'} &= -\frac{g_{\text{B-L}}}{3}\cos\theta'_W + \frac{g}{2}\cos\theta_W \sin\theta'_W - \frac{g_{\mathrm{Y}}}{6}\sin\theta_W\sin\theta'_W - \frac{g_{\mathrm{YB}}}{3}\sin\theta_W\sin\theta'_W \,, \\ g_{\mathrm{R}}^{ttZ'} &= -\frac{g_{\text{B-L}}}{3}\cos\theta'_W - \frac{2g_{\mathrm{Y}}}{3}\sin\theta_W\sin\theta'_W - \frac{g_{\mathrm{YB}}}{3}\sin\theta_W\sin\theta'_W \,. \end{aligned} \tag{3.42}$$

The loop integral $\mathrm{T}_7\left(m_{Z'}^2, m_t^2, m_t^2\right)$ was determined in Ref. [32] and, in the limit $m_{Z'} \gg m_t$, as we show in Eq. (**??**), it gets simplified to

$$\mathrm{T}_7\left(m_{Z'}^2, m_t^2, m_t^2\right) \simeq \frac{2}{m_{Z'}^2} \,, \tag{3.43}$$

up to a small truncation error (see Appendix **??** for details). For the parameter space region under consideration the difference $g_{\rm L}^{ttZ'} - g_{\rm R}^{ttZ'}$ can be cast in a simplified form as follows

$$\left(g_{\rm L}^{ttZ'} - g_{\rm R}^{ttZ'}\right) \simeq \frac{\left(g^2 + g_{\rm Y}^2\right) g_{\rm YB}}{32 g_{\rm B\text{-}L}} \left(\frac{v}{x}\right)^2 . \tag{3.44}$$

Using this result and the approximate value of the loop factor, we can calculate the ratio between the two- and one-loop contributions to the muon $(g-2)_\mu$,

$$\frac{\Delta a_\mu^{\gamma Z'}}{\Delta a_\mu^{Z'}} \simeq -\frac{g^2 g_{\rm Y^2}}{2048\pi^2} \frac{g_{\rm YB}}{g_{\rm B\text{-}L}} \left(\frac{v}{x}\right)^2 \ll 1 , \tag{3.45}$$

which shows that $\Delta a_\mu^{\gamma Z'}$ does indeed play a subdominant role in our analysis and can be safely neglected.

3.3 The B-L-SM Conclusions

In this chapter, we have confronted the model with the most recent experimental bounds from the direct Z' boson and next-to-lightest Higgs state searches at the LHC. Simultaneously, we have analysed the prospects of the B-L-SM for a consistent explanation of the observed anomaly in the muon anomalous magnetic moment $(g-2)_\mu$. Done through exploring B-L-SM potential for the observed $(g-2)_\mu$ anomaly in the regions of the model parameter space that are consistent with direct searches and electroweak precision observables.

As one of the main results of our analysis, we have found phenomenologically consistent model parameter space regions that simultaneously fit the exclusion limits from direct Z' searches and can explain the muon $(g-2)_\mu$ anomaly. We have distinguished four benchmark points for future phenomenological exploration at experiments, the first one with the lightest allowed Z' ($m_{Z'} > 3.1$ TeV), the second with the lightest additional scalar boson ($m_{h_2} > 400$ GeV), and the other two points that reproduce the muon $(g-2)_\mu$ anomaly within 1σ uncertainty range. Besides, we have studied the correlations of the Z' production cross section times the branching ratio into a pair of light leptons versus the physical parameters of the model. In particular, we have found that the muon $(g-2)_\mu$ observable dominated by Z' loop contributions lies within the phenomenologically viable parameter space domain. For completeness, we have also estimated the dominant contribution from the Barr-Zee type two-loop corrections and found a relatively small effect.

Chapter 4

3HDM

4.1 Pre-3HDM

The properties of the new resonance observed at the LHC in 2012 [ ] seem tantalizingly close to those of the Higgs boson predicted by the Standard Model (SM) (for instance, see [ ]) (...) Typical BSM scenarios that aim to fix one or more such shortcomings of the SM often end up extending the scalar sector of the SM. In these extensions, the 125 GeV scalar observed at the LHC is not the only scalar in the spectrum but the first one in a series of others to follow.

This is an intriguing possibility which motivates us for a closer inspection of the properties of the observed scalar and inspires us to carry on our efforts to look for new resonances at the collider experiments.

This is often done by adding to the SM simple replicas of the SM doublet, without altering the EW VEV. The first, and unsurprisingly simplest, of these kinds of models was presented in 1973 in [ ] as a means to obtain a spontaneous breaking of the CP symmetry, and boast a rich phenomenology. Along with richer phenomelogy the existence of a charged Higgs Boson allows for other phenomena to occur. Explain

4.2 BGL? Should I meantion it

The BGL model was a version of one of these 2HDM models where the scalar interactions with fermions explicitly violate flavour families. This akin to what the W boson does on the SM. This is usually avoided trough the creation of a additional Z_2 or a U_1 symmetry [ ]. This forces each fermion of the same charge to couple to a single doublet, thereby preventing FCNC.

We already discussed some of the reasons why these symmetries are imposed. These tree-level mediated FCNCs would make significant contributions to the flavour sector observables, such as meson masses or the flavour decays and ratios. This would destroy the agreement with experimental observations.

Unless the masses of the new scalars are all of order TeV, or the FCNC Yukawas couplings are fine-tuned to be very small.

These models are meantioned here for the simple fact they propose the reason why the flavour observables are suppresed is through a aditional impossed symmetry. Thus providing a natural explination to why NP contributions to the flavour observables are to be in agreement with the SM.

4.2.1 Lagrangian Yukawa

If we observe the quark section of the 2HDM model. We have

$$\mathcal{L}_Y \supset \sum \tag{4.1}$$

where $Q_L^a = (p_L^a n_L^a)^T$ and ϕ_i are the SU(2) weak isospin quark and Higgs doublets respectively. Here we also introduce the fields n and p these are the positive and negatively charged under the $\mathcal{Z}_2$ symmetry quark fields. With a, b being the family indexes for the fermion families. We have two yukawa matrices here, the coupling to the up and down sector respectively.

Upon SSB the vaccum value of each doublet will take the shape of $\frac{v_1}{\sqrt{2}}$ and $\frac{v_2}{\sqrt{2}}$ with their sum being $246GeV$. We define $\tan(\beta) = \frac{v_1}{v_2}$.

For a CP-conserving model we must introduce a charged scalar H^+ , a pseudoscalar A and two CP-even scalars h and H.

Upon rotation to the mass basis we get the mass matrices for quarks to be,

$$M_p \frac{1}{\sqrt{2}} (D_1 v1 + D_2 v_2) \quad \frac{1}{\sqrt{2}} (\Gamma_1 v_1 + \Gamma_2 v_2) \tag{4.2}$$

The eigenvalues of which will have to be the physical quakr masses. Through the same bi-unitary procedure we used earlier we can write,

$$\begin{aligned} D_u &= V_L^\dagger M_p V_R = diag\{m_u, m_c, m_t\} \\ D_d &= U_L^\dagger M_n U_R = diag\{m_d, m_s, m_b\} \end{aligned} \tag{4.3}$$

where m˙x are the phsycial quark masses. These matrices like before will relate the quark states to their original fields as,

$$\begin{aligned} p_L &= V_l u_L \quad p_R \\ n_L &= \quad n_R \end{aligned} \tag{4.4}$$

The CKM matrix is then obtained as

$$V = V_L U_L^\dagger \tag{4.5}$$

We also define the following matrices,

$$\begin{aligned} N_u &= \frac{1}{\sqrt{2}} \\ N_d &= \frac{1}{\sqrt{2}} \end{aligned} \tag{4.6}$$

which end up related to the Yukawa couplings between the physical scalars and quarks. Through these we can write the lagrangian portion of the BGL lagrangian as

$$\mathcal{L}_Y = \frac{iA}{v} + \frac{h}{v} \overline{u} \tag{4.7}$$

You can see how the lagraiang above the aligment limit is when the lightr higgs Yukawa interactions are exactly those of the SM particles. In fact if one imposses $\sin(\beta - \alpha) = 1$ this forces the vertices between h and the electroweak gauge bososns to be exactly those of the SM Higgs particle.

In models with flavour conservation, each family of fermions of the same electrical charge couple to a single Higgs Doublet via the impossition of the Z2 or U1 symmetry. So the diagonalization of mass matrices seen is the same as the diagonalization of the N_u and N_d matrices. This means that there will be no flavour violating yukawa interaction mediated by the neutral scalalars. In general it is thought that will not be case and that some FCNCs occour at the tree level.

The BGL model is based on a symmetry impossed on the whole lagrangian that will in a sense affect only the quark and scalar fields.

$$Transforms of fields here. \tag{4.8}$$

in fact there are 6 possible choices here, depending on which family we take to be the one that transforms under these rotations. The choise we'll examine is the one where as you can see by the 4.8, is the one were the first generation of quarks is afected and this yields a peccei-Quinn scalar potential which must be complemented with a soft breaking paramater to yield a massive pseudocalar particle.

The dfermion sector sees the impasct of this transformation by a set of several! entries in the yukawa matrices that have to be set to zero.

$$Showingtheyukawamatrices. \tag{4.9}$$

Here x marks a generic non-zero entry. The form of these matricies imply a shape for the Matrix Mp that is block diagonal as,

$$Showingthemassmatrix. \tag{4.10}$$

Also shaping the bi-diagonalized matrices V_L and V_R to be,

$$V_L = \quad V_R = \tag{4.11}$$

with some phase θ_r. The shapes seen here are crucial for FCNC supression. I didn't understand but our choice leads to no FCNCs in the up sector.

By showing a load of stuff we can see that in this case! Thus we see that the off-diagonal Yukawa couplings between scalars and down-type quarks which are indeed the strength of the FCNC interactions are CKM-suppressed.

There is a freedom to choose the "1" family as any one of the physical quark generations, and therefore one has three BGL models with FCNC in the down sector and without it in the up sector. An analogous symmetry to that of eq. (8) yields another three models, where FCNC now occurs associated with a given family of up-type quarks but where no FCNC occurs for down-type quarks.

This then is how the hallmark of the BGL models is achieved: a flavour-breaking symmetry, which yields off- diagonal FCNC couplings naturally suppressed by the entries of the CKM matrix elements. We will now build a similar model, but with three Higgs doublets

4.3 General Notes

4.3.1 Basic

Here we discuss the construction a three Higgs doublet model with a flavour non-universal U(1) × Z_2. This symmetry will suppress the flavour changing interactions mediated by neutral scalars.

such a model can thus encourage direct searches for extra Higgs bosons in the future collider experiments, and includes a non-trivial flavour structure.

Beyond the simply aesthetic considerations of having 3 higgs doublets as we have 3 generations of fermions there is a large range of reasons why the attempt of a 3HDM with similar supression of FCNCs as in theBGL models. (which?)

The BGL model was quite unique and sucessful but recent studies have shown that it's paramater space is quite limited. Althought these studies did not consider the leptonic sector and how these sectors interact with the extended scalar family [ ]

BGL models have enough freedom to have a flavour-preserving leptonic sector in what concerns the scalars, which is what we will consider here. Nonetheless, this shows that even with natural FCNC coupling suppression via off-diagonal CKM matrix elements.

4.4 Formulation of the 3HDM-BGL like model

4.4.1 The scalar potential

The scalar doublets are made to transform under the $U(1) \times Z_2$ symmetry as follows:

$$Transformations \tag{4.12}$$

We must require the scalar potential to be CP-invraiant, this means to be invariant under CP transformations.

$$moretransformations \tag{4.13}$$

Then given this the scalar potential takes shape,

$$V(\phi) \tag{4.14}$$

Where due to the CP symetry all paramaters are real. We have introduced a real soft breaking term with the paramater μ to avoid the apperence of a mssless axion. The same process as in the 2HDM BGL due to the similar breaking of the $U(1)$ symmetry.

All doublets aquire the same shape after their VEV aquisition,

$$VEVShape \tag{4.15}$$

where vk represnets the VEV of each doublet, these must satisfy the condition $\sum = (246GeV)^2$ The minimization of the potential yields three equations which means that one can epxress the quadratic poarameters μ_i in favour of these VEV and couplings as,

$$\mu_s eqs \tag{4.16}$$

We also parameterize the VEVs as

$$vs = \tag{4.17}$$

where v is just the value of the electroweak vev. The orthogonal matrix,

$$\mathcal{O} \tag{4.18}$$

Will simplify our analysis of the charged and pseudoscalar sectors. We turn our attention to the physical scalar spectrum of the model. Since we are considering a potential with explicit CP ocnservation and a vacum who does not break CP. the neutral scalars have definite CP quantum numbers and the scalar spectrum of the model is composed of a trio of cP even scalars and a pair of charged scalars.

The CP-odd scalar sector

The CP-even or charged scalar sector

4.4.2 The Yukawa sector

4.4.3 The inverse procedure and the Quark masses

4.5 Constraints on the Model

4.6 Numerical Results

Higgs Plots

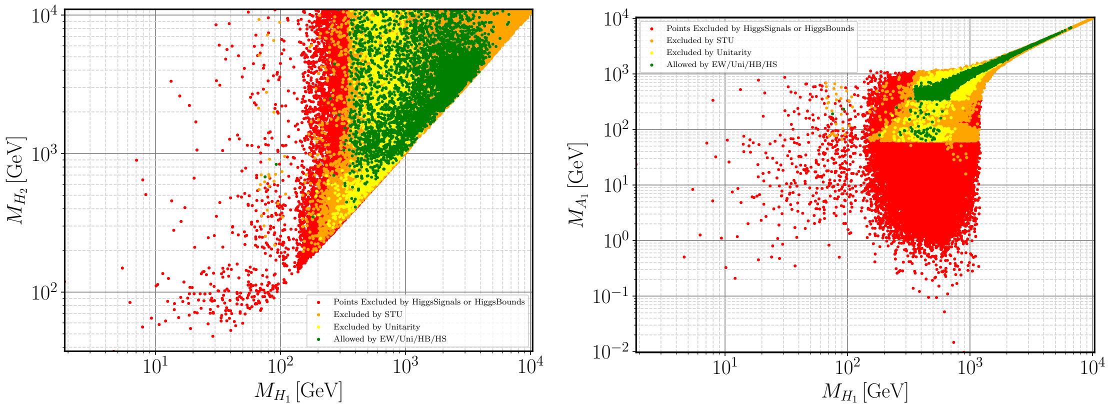

Figure 4.1: Scatter plots of parameter space allowed under several cuts imposed on the BGL-like 3HDM. Right we have the plot showing the masses of the two heavier CP-even scalars H_2 and H_1 while in the right we show the relation between the lightest (non-h) of the CP-even and pseudoscalar particles. Red points failed HS and HB tests; yellow points violate unitarity constraints; orange points only fail electroweak precision constraints, and green ones satisfy all restrictions.

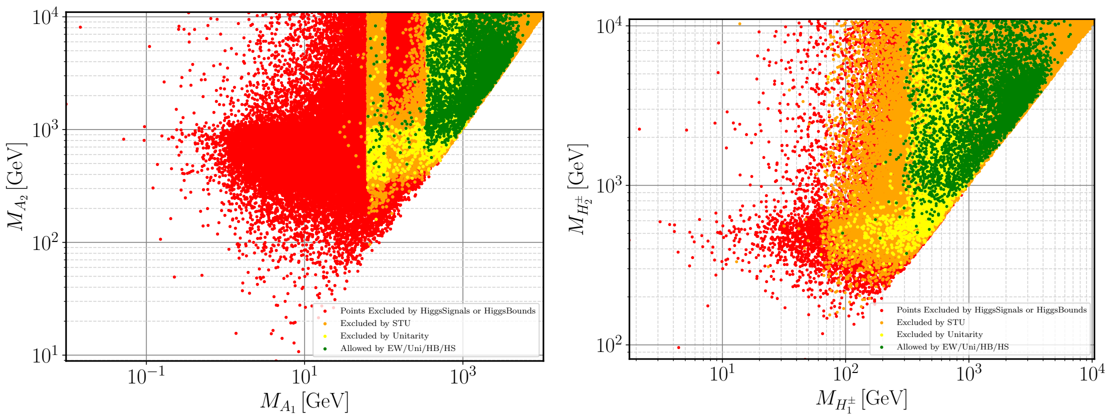

Figure 4.2:

4.6.1 Flavour results

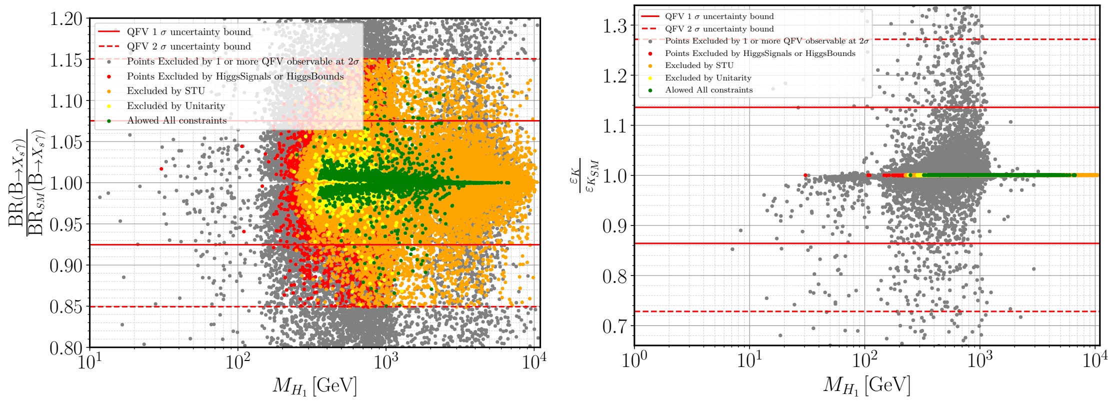

Figure 4.3: Scatter plots of parameter space allowed under several cuts imposed on the BGL-like 3HDM. Right we have the plot showing the masses of the two heavier CP-even scalars H_2 and H_1 while in the right we show the relation between the lightest (non-h) of the CP-even and pseudoscalar particles. Red points failed HS and HB tests; yellow points violate unitarity constraints; orange points only fail electroweak precision constraints, and green ones satisfy all restrictions.

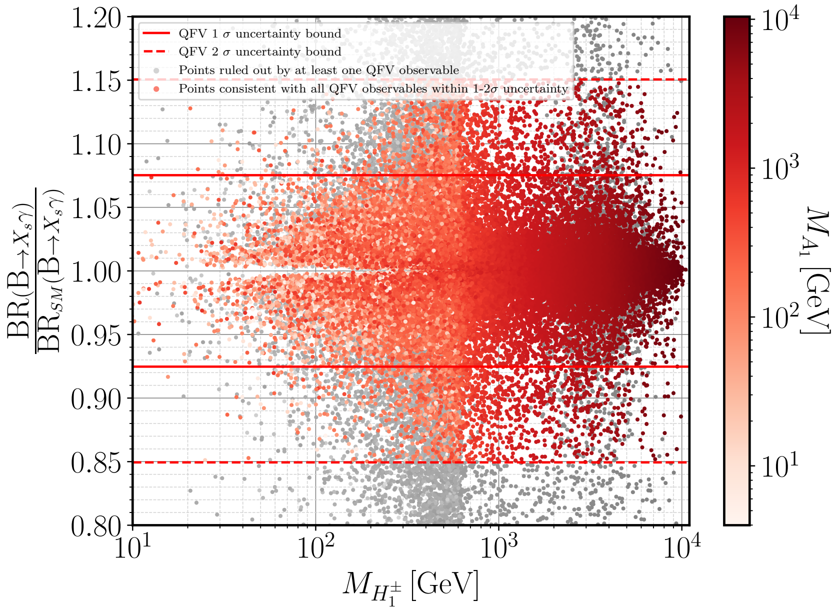

Figure 4.4:

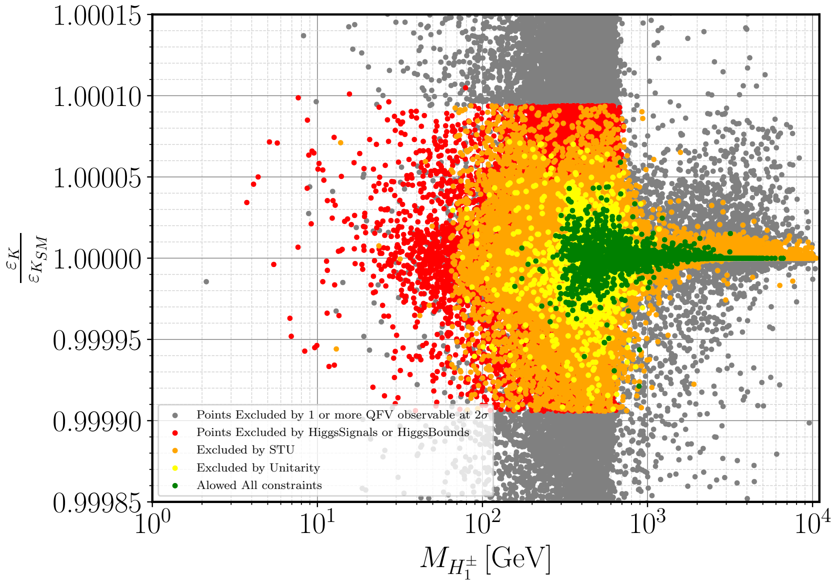

Figure 4.5:

Fine-Tuning

4.6.2 Conclusions

New scalars with masses below the TeV scale can still successfully negotiate the constraints arising from flavour data.

4.7 Old

We have studied the main features and the phenomenological consistency of a family non-universal Three Higgs Doublet Model or 3HDM with a softly broken $\mathrm{U}(1) \times \mathrm{Z}_2$ symmetry group. This broken symmetry will justify the flavour hierarchies in the SM and trough a Branco-Grimus-Lavoura mechanism supress the otherwise expected Flavour Changing Neutral Currents.

Let us now consider an extended version of the SM, with an enlarged Higgs sector that contains three generations of scalar-doublets. These Higgs will be named ϕ^i with $i = 1, 2, 3$. In this sector we must enforce the alignment limit to the scalar sector ensuring the physical scalar spectrum accommodates a SM-like Higgs boson with mass of 125.09 GeV.

Chapter 5

Future Work

Chapter 6

Appendix

6.0.1 Gamma Matrices

The γ matrices are defined as,

$$\{\gamma^\mu, \gamma^\nu\} = 2g^{\mu\nu} I \tag{6.1}$$

where,

$$g^{\mu\nu} = \begin{pmatrix} 1 & 0 & 0 & 0 \\ 0 & -1 & 0 & 0 \\ 0 & 0 & -1 & 0 \\ 0 & 0 & 0 & -1 \end{pmatrix} \tag{6.2}$$

and if $\gamma_\mu = (\gamma^0, \gamma)$ then it is usual to require for the hermitian conjugate matrices,

$$\gamma^{0\dagger} = \gamma^0 \quad \text{and} \quad \gamma^\dagger = -\gamma \tag{6.3}$$

6.0.2 Lagrangian Dynamics

In Lagrangian dynamics we define the action S has,

$$\mathcal{S} = \int L \, dt = \int \mathcal{L}(\phi, \partial\phi) \, d^4x \tag{6.4}$$

where L is the Lagrangian, and the $\mathcal{L}$ is designated as the *Lagrangian density*, note these terms are usually used interchangeable. Here $\mathcal{L}$ is a function of the field ϕ and it's spatial derivatives.

The action S is constrained by the principle of least action, this requires the "path" taken by a field between an initial and final set of coordinates to leave the action invariant, this can be expressed by,

$$\partial\mathcal{S} = 0 \tag{6.5}$$

from here one can deduce the *Euler-Lagrange* equations,

$$\partial_\mu \left(\frac{\partial\mathcal{L}(\phi, \partial\phi)}{\partial(\partial_\mu)} \right) - \frac{\partial\mathcal{L}(\phi, \partial\phi)}{\partial\phi} = 0 \tag{6.6}$$

Bibliography

[1] M. Aaboud *et al.*, "Search for new high-mass phenomena in the dilepton final state using 36 fb^{-1} of proton-proton collision data at $\sqrt{s} = 13$ TeV with the ATLAS detector," *JHEP*, vol. 10, p. 182, 2017.

[2] R. N. Mohapatra and R. E. Marshak, "Local B-L Symmetry of Electroweak Interactions, Majorana Neutrinos and Neutron Oscillations," *Phys. Rev. Lett.*, vol. 44, pp. 1316–1319, 1980. [Erratum: Phys. Rev. Lett.44,1643(1980)].

[3] L. Basso, S. Moretti, and G. M. Pruna, "Constraining the g'_1 coupling in the minimal $B-L$ Model," *J. Phys.*, vol. G39, p. 025004, 2012.

[4] L. Basso, S. Moretti, and G. M. Pruna, "Theoretical constraints on the couplings of non-exotic minimal Z' bosons," *JHEP*, vol. 08, p. 122, 2011.

[5] M. Tanabashi *et al.*, "Review of Particle Physics," *Phys. Rev.*, vol. D98, no. 3, p. 030001, 2018.

[6] M. S. Chanowitz, J. R. Ellis, and M. K. Gaillard, "The Price of Natural Flavor Conservation in Neutral Weak Interactions," *Nucl. Phys.*, vol. B128, pp. 506–536, 1977.

[7] H. Fritzsch and P. Minkowski, "Unified Interactions of Leptons and Hadrons," *Annals Phys.*, vol. 93, pp. 193–266, 1975.

[8] H. Georgi and D. V. Nanopoulos, "T Quark Mass in a Superunified Theory," *Phys. Lett.*, vol. 82B, pp. 392–394, 1979.

[9] H. Georgi and D. V. Nanopoulos, "Ordinary Predictions from Grand Principles: T Quark Mass in O(10)," *Nucl. Phys.*, vol. B155, pp. 52–74, 1979.

[10] H. Georgi and D. V. Nanopoulos, "Masses and Mixing in Unified Theories," *Nucl. Phys.*, vol. B159, pp. 16–28, 1979.

[11] Y. Achiman and B. Stech, "Quark Lepton Symmetry and Mass Scales in an E6 Unified Gauge Model," *Phys. Lett.*, vol. 77B, pp. 389–393, 1978.

[12] F. Gursey, P. Ramond, and P. Sikivie, "A Universal Gauge Theory Model Based on E6," *Phys. Lett.*, vol. 60B, pp. 177–180, 1976.

[13] F. Gursey and M. Serdaroglu, "E6 GAUGE FIELD THEORY MODEL REVISITED," *Nuovo Cim.*, vol. A65, p. 337, 1981. [,271(1981)].

[14] T. Yanagida, "Horizontal gauge symmetry and masses of neutrinos," *Conf. Proc.*, vol. C7902131, pp. 95–99, 1979.

[15] M. Gell-Mann, P. Ramond, and R. Slansky, "Complex Spinors and Unified Theories," *Conf. Proc.*, vol. C790927, pp. 315–321, 1979.